

THESIS

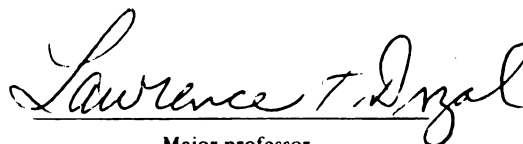
1
(1996)



This is to certify that the
thesis entitled
DEVELOPMENT OF A HIGH SPEED POWDER
PROCESS TO MANUFACTURE COMPOSITE
PREPREG

presented by
MURTY N. VYAKARNAM

has been accepted towards fulfillment
of the requirements for
MASTER'S degree in SCIENCE


Major professor

Date NOVEMBER 20, 1992

0-7639

MSU is an Affirmative Action/Equal Opportunity Institution



PLACE IN RETURN BOX to remove this checkout from your record.
TO AVOID FINES return on or before date due.

DATE DUE	DATE DUE	DATE DUE
_____	_____	_____
_____	_____	_____
_____	_____	_____
_____	_____	_____
_____	_____	_____
_____	_____	_____
_____	_____	_____

MSU Is An Affirmative Action/Equal Opportunity Institution

c:\circ\dstduea.pm3-p.1

**DEVELOPMENT OF A HIGH SPEED POWDER
PROCESS TO MANUFACTURE COMPOSITE
PREPREG**

By

Murty N. Vyakarnam

A THESIS

Submitted to
Michigan State University
in partial fulfillment of the requirements
for the degree of

MASTER OF SCIENCE

Department of Chemical Engineering
Composite Materials and Structures Center

1992

ABSTRACT

DEVELOPMENT OF A HIGH SPEED POWDER PROCESS TO MANUFACTURE COMPOSITE PREPREG

By

Murty N. Vyakarnam

A High Speed Powder Process has been developed to manufacture unidirectional prepreg tapes of any desired volume fraction matrix based on the prototype Powder Process developed at Michigan State University.

In this investigation, the limitations in operating the prototype at higher speeds were analyzed. This led to the development of a vertical configuration of the process in which the aerosol is generated independently and transported into a novel counter current contacting chamber from the top while spread fibers enter from the bottom. Research into the aerosolization characteristics of polymer powder matrices has resulted in optimizing the design of the impregnation chamber, designing a gas distributor ring and a nozzle for efficient aerosol generation and entrainment, and determining the operating curves for estimating the volume fraction of matrix in the prepreg. A tension sensor was also incorporated in the process to minimize fluctuations in the fiber motion.

The process has been successfully demonstrated for the AS4 carbon fiber - polyamide powder matrix system at economically viable speeds of 20 cm/s and greater.

Copyright by
Murty N. Vyakarnam
1992

In loving memory of my father

ACKNOWLEDGEMENTS

I would like to thank Dr Lawrence T. Drzal for his constant guidance and leadership which encouraged and inspired me in developing the process.

The development of the process was an outcome of the fundamental work done by Dr. Shri R. Iyer. I gratefully acknowledge his contribution in the advancement of composite prepreg processing. I thank Sanjay for his valuable suggestions from time to time which contributed in a big way in making the process a success. I am also indebted to James for the contributions he made in building and operating the process.

The High Speed Powder Process would not have shaped up in the CMSC facility without the excellent infrastructural support and cooperation provided by Mike Rich. My thanks are also to Brian Rook for helping me set up various equipment. I appreciate the prompt and efficient services provided by the DER Machine Shop personnel especially Mike. Pete Walalauge of the IDC Corporation deserves special thanks for trouble shooting the control system and keeping the downtime of the process to a minimum.

I am thankful to all my friends and family members who have been a constant source of support and encouragement. Lastly, I would thank my mother who always inspired me to do better things in life.

Table of Contents

List of Tables	. .	viii
List of Figures	. .	ix
1. Introduction	. .	1
1.1 Background	. .	2
1.2 MSU Powder Process	. .	8
1.3 Thesis Objective	. .	10
2. Aerosolization Characteristics of Polymer Powders	. .	12
2.1 Introduction	. .	12
2.2 Review of Cohesivity and Tribocharging of Polymer Powders	. .	13
2.3 Powders Investigated	. .	19
2.4 Experimental Setup	. .	25
2.5 Results and Discussion	. .	27
2.6 Summary	. .	38
3. Process Design	. .	39
3.1 Introduction	. .	39
3.2 Process Design Criteria	. .	39
3.3 Development of Process Scheme	. .	41
3.4 Spreader	. .	44
3.5 Aerosol Generator	. .	45
3.5 Impregnation Chamber	. .	48
3.7 Heater	. .	51
3.8 Summary	. .	52
4. Process Control	. .	55
4.1 Introduction	. .	55
4.2 Fiber Motion	. .	56
4.3 Line Speed Control	. .	59
4.4 Temperature Controller	. .	62
4.5 Process Variables	. .	65

4.6 Summary	..	66
5. Prepreg Processing	..	67
5.1 Materials	..	67
5.2 Spreader Performance	..	68
5.3 Aerosol Generation	..	70
5.4 Process Runs	..	73
5.5 Sintering Operation	..	76
5.6 Summary	..	76
6. Conclusions	..	79
Bibliography	..	82

List of Tables

Table 1.1	Typical Reinforcing Fibers ^[3]
Table 1.2	High Performance Polymers ^[4,5]
Table 2.1	Triboelectric Series of Polymer Materials ^[23]
Table 2.2	Powders Investigated for Aerosolization Characteristics
Table 5.1	Fiber - Matrix Material Properties
Table 5.2	Summary of High Speed Prepreg Process Runs
Table 5.3	Typical Analysis of a Process Run

List of Figures

- Figure 1.1** Electrostatic Fluidized Bed
- Figure 1.2** Forced Air Impregnation Process
- Figure 1.3** MSU Powder Prepreg Process
- Figure 2.1** Classification of Powders based on Fluidization Behavior ^[18]
- Figure 2.2** SEM Micrographs of Polyamide Powders - Typical Distributions and Surface Characteristics (5 μ and 10 μ powders)
- Figure 2.3** SEM Micrographs of Polyamide Powders - Typical Distributions and Surface Characteristics (20 μ and 65 μ powders)
- Figure 2.4** SEM Micrographs of PEEK Powder - Typical Distribution & Surface Characteristics and Impregnation on Carbon Fiber
- Figure 2.5** Experimental Setup to Determine Aerosolization Characteristics
- Figure 2.6** Momentum Balance in Aerosolization Chamber ^[4]
- Figure 2.7a** Effect of Bed Weight on the Resonant Frequency of Small Aerosolizer (Glass Spheres)
- Figure 2.7b** Effect of Bed Weight on the Resonant Frequency of Big Aerosolizer (Polyamide 5 μ m Powder)
- Figure 2.8** Variation of Particle Entrainment with Gas Flow Rate
- Figure 2.9** Gas Distributor Ring
- Figure 2.10** Effect of Gas Distributor on Particle Entrainment
- Figure 3.1** Economic Analysis of Powder Process^[17]

- Figure 3.2** Schematic of the High Speed Powder Prepreg Process
- Figure 3.3** Schematic of Spreader
- Figure 3.4** Features of Aerosol Generator
- Figure 3.5** Impregnation Chamber
- Figure 3.6** Heater for Sintering Operation
- Figure 4.1** Process Control Strategy of the Process
- Figure 4.2** Schematic of the Tension Control System
- Figure 4.3** Oven Temperature Profile
- Figure 4.4** Temperature Control Circuit for Oven
- Figure 5.1** Effect of Speed and Amplitude on Spreading
- Figure 5.2** Aerosol Generation Characteristics - Constant Nozzle Flowrate
- Figure 5.3** Aerosol Generation Characteristics - Constant Distributor Flowrate
- Figure 5.4** SEM Micrographs of AS4 Carbon - Polyamide Prepreg

Chapter 1

Introduction

Composite materials are a combination of two or more physically and/or chemically distinct materials resulting in mechanical or other property performance superior to the individual constituents. These materials are generally (i) Fibrous; (ii) Laminate; or (iii) Particulate; depending upon the physical state of the reinforcing material and the matrix [1]. The dispersion of the different components in the composite material must be controlled to achieve optimum properties. Prepreg tape is a precursor composite form that aids the fabrication of a continuous fiber composite material. Iyer and Drzal [2] developed a novel dry powder process for inexpensively making prepreg tape. The successful performance of a laboratory prototype led to the development of a scaled-up version, with a prepregging rate an order of magnitude higher than the prototype in order to validate the operating models. This dissertation focuses on the development of the high speed powder process prototype to manufacture unidirectional prepreg tape.

The selection of fibers and matrices for a composite material are finally dictated by the end use properties, fiber matrix interface and processability. In polymer composites the reinforcing fibers are usually carbon, glass or Kevlar. Typical high performance fibers and their properties are listed in Table 1.1 [3]. The matrix in a

prepreg tape is an unconsolidated polymer which can be either a thermoplastic or a thermoset. Thermoset matrices such as epoxies are used because of low shrinkage, excellent adhesion, and good chemical resistance. However, thermoset tapes have the disadvantages of limited shelf life, low resin strength, low fracture toughness, high degree of brittleness, tendency to degrade at high temperatures and cold storage requirements to prevent additional curing. On the other hand, thermoplastic matrices have certain advantages over thermoset resins. These include short molding cycle time, infinite shelf life of prepreg tape, better fracture toughness, capability of fusion bonding, recyclability, repairability, increased moisture resistance, and reduced storage and handling problems. Nonetheless, processing problems are encountered in the making of thermoplastic prepreg tapes because of their high viscosities. Table 1.2 lists common thermoplastic resins [4,5].

1.1 Background

A literature survey in the area of composite prepreg manufacture has shown that various processes have been developed since 1962. The mode of matrix impregnation and the salient features of each of these processes are reviewed in this chapter.

1.1.1 Slurry Process

In this process, Taylor [6] passed fiber tow through a slurry tank containing the polymer in suspension in a liquid carrier. Polymer particles are trapped within the fiber

Table 1.1 Typical Reinforcing Fibers ^[3]

Fiber Type	Specific Gravity	Young's Modulus E (GPa)	Strength (GPa)	Diameter (μm)	Highest Usable Temperature $^{\circ}\text{C}$
E Glass	2.5 - 2.6	69 - 72	1.7 - 3.5	5 - 25	350
S Glass	2.48	85	4.8	5 - 15	300
Carbon HM	1.96	517	1.86	8 - 14	600
Carbon HS	1.8	295	5.6	5.5	500
Kevlar 49	1.45	135	3	12	250

Table 1.2 High Performance Polymers ^[4,5]

Polymer	Trade Name	Glass Transition Temperature, $^{\circ}\text{C}$	Melt Temperature $^{\circ}\text{C}$
Polyamide	Atochem-Organosol	42	175 - 180
Poly ether ether ketone	ICI-Victrex PEEK	143	343
Polyether ketone ketone	DuPont-PEKK	156	338
Polyphenylene sulfide	Ryton PPS	90	285
Thermoplastic imide	LARC - TPI	217 - 229	275 - 305
Polyamide imide	Torlon C	275	None

tow. This impregnated tow is dried in a drying chamber before passing through a heater to be wound on a take up spool. O'Conner [7] reported that some of the problems encountered in this technique include finding the right concentration of slurry and maintaining the optimum concentration in the resin tank besides the time consuming drying step prior to consolidation to ensure there is no liquid remaining that can lead to voids in the final composite.

1.1.2 Solution Process

Turton et al. [8] developed a process in which low viscosity solution of the thermoplastic/thermoset material is made by dissolving it in a solvent and fiber tow is impregnated by passing it through this solution. Complete removal of the solvent is a difficult, stringent and time consuming step. Epoxies, polyimides, polysulfones are some of the matrices that have been solution impregnated.

1.1.3 Melt Impregnation

Prepreg tapes are produced by passing the fiber tow through a molten polymer. In the case of thermosets, processing by this method is feasible when temperature and reaction kinetics allow for continuous impregnation. In the case of thermoplastics viscosity of the melt is a major problem and forces exerted to pull the fibers are often so high that fiber damage occurs. Thermal degradation of the polymer may also become a problem. Two approaches have been used in processing the thermoplastics, (i) a cross head extruder feeds molten polymer into a die through which the rovings pass [9], and

(ii) fibers pass through a molten resin bath fitted with impregnation pins [10]. The resulting prepreg tape by this method usually lacks tack and drape.

1.1.4 Film Stacking

In this process layers of the reinforcing fibers either in the form of unidirectional tows or woven fabric are stacked with thermoplastic sheets and consolidated under pressure for long times. This process is widely used with low viscosity materials [11]. Disadvantages include high resin content, difficulty in impregnating the fiber tow (high pressure forces the fibers together) with high viscosity material besides being labor intensive.

1.1.5 Fiber Commingling

In this technique a co-mingled hybrid yarn consisting of the thermoplastic yarn and the reinforcing fiber tow is produced. These hybrid yarns are then consolidated to form composite parts [12]. While drapeability of the hybrid yarn is a distinct advantage, high costs are involved in producing the thermoplastic yarn and weaving it with the reinforcing fibers.

1.1.6 Foam Process

Chary et al. [13] developed a technique to continuously coat carbon fibers using aqueous foam. The process may be an attractive alternative to the slurry process, where

significant drying time is required. Nonetheless, the removal of the surfactant from the fiber-matrix system is a difficult and time consuming task.

1.1.7 Dry Powder Impregnation

Dry powder impregnation was first developed by Price [14] in which glass roving was passed through a bed of thermoplastic powder viz. polypropylene. The particles stick to the fibers due to natural electrostatic attraction. This tow is then heated and passed through a die to obtain an impregnated tow. Spreading of tow is not achieved, hence this technique is restricted to producing short fiber reinforced composites. Tight control over the matrix volume fraction is also not possible. Later, three dry powder processes using different approaches were developed concurrently by Muzzy et al. [15], Allen et al. [16] and Iyer et al. [2,4]. Dry powder processes offer the potential for creation of a high speed, low cost process with controllable matrix volume fraction.

1.1.7.a Electrostatic

Muzzy et. al. [15] developed a process to manufacture powder prepreg using an electrostatic fluidized bed of PEEK powder (Figure 1.1). The fiber tow passes through a spreader and then through an electrostatic fluidized bed of polymer powder of 10 - 250 microns in size. The imposed electrostatics ensure that the particles adhere to the fibers and is necessary for the large particles used in the process. However, an electrostatic fluidized bed has to solve the problem of agglomeration and channeling faced by conventional techniques before it is applicable to the fluidization of smaller particle sizes.

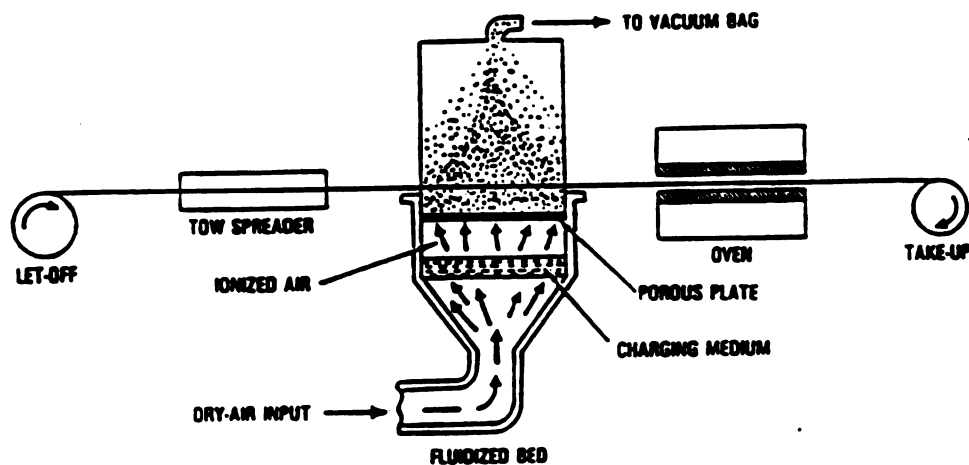


Figure 1.1 Electrostatic Fluidized Bed Process

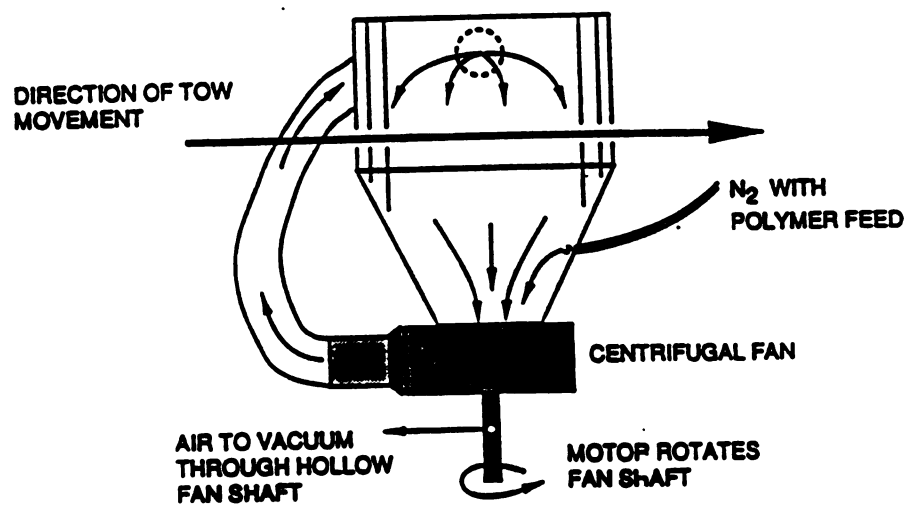


Figure 1.2 Forced Air Impregnation Process

1.1.7.b Forced Air Impregnation

Allen et al. [16] impregnated the fibers in a recirculating powder deposition chamber with annular walls for powder recovery (Figure 1.2). The chief drawback in this process lies in the control. Humidity of the environment, material balances in the chamber to decide feed rates, pressure drop in the recirculating tubes to prevent clogging and the cohesive nature of fine powders make process control a very difficult task, especially at particle concentrations in excess of 10,000 mg/m³.

1.2 MSU Powder Process

Iyer et al. [2,4] developed a powder prepreg process which involves the passing of spread fibers through an aerosol of polymer particles generated by acoustic means. This process is capable of producing prepreg tapes where each fiber is intimately wetted by the polymer matrix and offers better control over the fiber-matrix volume fractions. No external means is used to charge the polymer powder. Instead the process relies on the tribocharging of the polymer particles to acquire high charge to mass ratios and to adhere to the spread reinforcing fibers. The principle in this process is that the average size of the polymer powder used should be approximately of the same order of magnitude in size as the reinforcing fiber. This principle was later confirmed by Padaki [5] who found the existence of an optimum particle size for the process in the same order of magnitude as the reinforcing fiber. The process is independent of matrix viscosity and does not use any solvents.

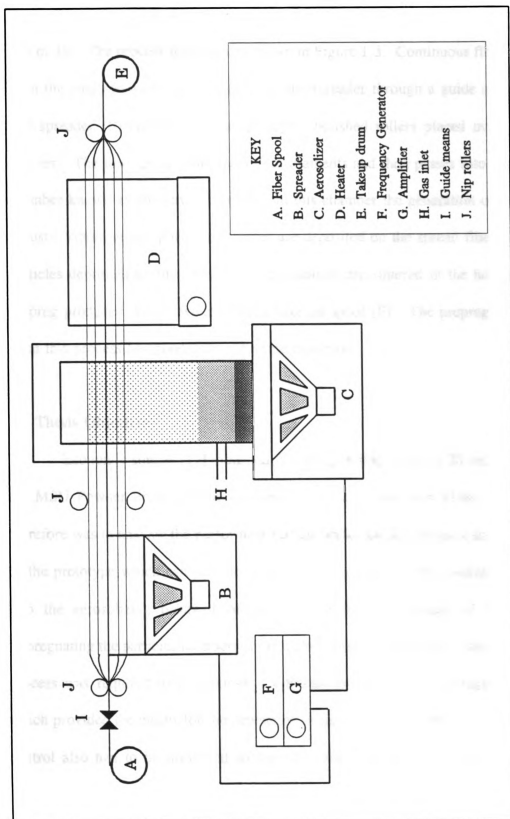


Figure 1.3 MSU Powder Prepreg Process

The prototype process was developed for an operating speed of 2 cm/s and a tow size of 3K. The process schematic is shown in Figure 1.3. Continuous fiber is unwound from the feed spool (A) and passed on to the spreader through a guide and nip rollers. The spreader (B) consists of a set of highly polished rollers placed over an acoustic speaker. The tow spreads into individual filaments and then passes into the deposition chamber known as the aerosolizer (C). In this chamber the generation of aerosol is by acoustic vibration and polymer particles are deposited on the spread fibers. Later, the particles deposited on the fibers in the aerosolizer are sintered in the heater (D). The prepreg produced is then wound on the take up spool (E). The prepreg tape obtained from this process has good tack and drape qualities.

1.3 Thesis Objective

Economic studies [17] indicated that an operating speed of 20 cm/s would allow the MSU Powder Process to be operated at a cost of less than \$1/lb. The objective therefore was to analyze the performance of the prototype and design a scaled up version of the prototype which can operate at 20 cm/s or greater. This involved investigation into the aerosolizing behavior of polymer powders and design of the means for impregnating the particles on fibers at the higher speed of operation. Modification to the process was required to incorporate a different design for the impregnation chamber which provided the means for the deposition of particles on the fibers. The fiber motion control also had to be improved so that the spreading efficiency was not lowered at

higher speeds of operation. The performance of the high speed process was evaluated for the carbon fiber-polyamide matrix system.

The thesis is divided into six chapters including the introduction. Aerosolization characteristics of polymer powders is discussed in the second chapter. The third chapter describes the development of the high speed process, its design and construction. Next, the process control aspects are discussed in Chapter 4. Chapter 5 deals with the performance of the high speed process. Chapter 6 summarizes the conclusions of this investigation with recommendations for future work.

Chapter 2

Aerosolization Characteristics Of Polymer Powders

2.1 Introduction

The polymer powders used in the process are typically below 100 microns in size. The small sizes of the particles and the low dielectric constants of these polymers make these powders cohesive (due to the presence of strong inter-particle forces) in nature and amenable to tribocharging. The phenomenon of tribocharging is beneficial to the impregnation process but is one of the less understood areas even today. Cohesivity of these powders requires special modes of aerosolization and poses certain processing problems like agglomeration during the course of operation. A brief review of the tribocharging concepts and the fluidization of cohesive powders is presented in this chapter.

Aerosolization characteristics of various powders were evaluated in order to make the powder process suitable for different matrix systems and to obtain design parameters for a scaled-up version of the process. Powders differing in size, density and shape were subjected to aerosolization studies in a small scale experimental set up. The effect of geometry on the efficiency of aerosolization was also probed. These semi-quantitative

geometry on the efficiency of aerosolization was also probed. These semi-quantitative studies gave the necessary understanding to design the scaled-up aerosol generator and the impregnation chamber.

2.2 Review of Cohesivity and Tribocharging of Polymer Powders

The behavior of the polymer powders with respect to aerosolization and impregnation on to the reinforcing fibers is important to the process. The required characteristics of the powders suitable for this process are:

- i) Ease in aerosolization
- ii) Ease in acquiring electrostatic charge
- iii) Size range about the same order of magnitude as the reinforcing fibers

The size range of polymer powders desirable for this process are also quite susceptible to acquiring a surface charge by triboelectrification thereby making them very cohesive and difficult to aerosolize. The process of aerosolization or dispersion of powders in a gaseous medium is akin to gas-solid fluidization in many respects. A literature review on aerosolization and fluidization indicated that considerable work has been done in the area of cohesivity of fine powders in recent years. Still a definite understanding of the underlying principles is lacking, especially for polymer powders. A brief review of these aspects is presented here.

2.2.1 Cohesive powders

Geldart [18] classified powders into A, B, C and D types based mainly on empirical observations (Figure 2.1). Type A powders are the most aeratable, while type B which are more coarse, do not fluidize homogeneously and are sand-like. Type C powders, which are of immediate interest with respect to this study, are generally finer than type A powders and are characterized by relatively strong cohesive forces. Type D powders are the coarsest of all and free flowing. Iyer and Drzal [19] classified the polyamide powders of sizes 12.2, 14.9, 19.4 microns as types C, AC and AC respectively.

Powder aerosolization is a balance between fluid dynamics forces, gravitational and inter particle forces (or cohesion). The dominant force of interaction between the particles in a powder is the omnipresent van der Waals force of attraction. Other attractive forces are capillary and electrostatic forces in the gaseous medium which are generally smaller than the van der Waals forces [20]. The separation distance between particles is critical in determining the van der Waals forces, since surface asperities or roughness can nullify this force if they increase the separation distance over 1 micron. The influence of each force can be related to the particle size 'r' [20].

Gravitational	$\propto r^3$
Van der Waals	$\propto r$
Electrostatic	$\propto r^2$
Capillary	$\propto r$

The above relationships indicate the strong dependence of the interacting forces on the particle size.

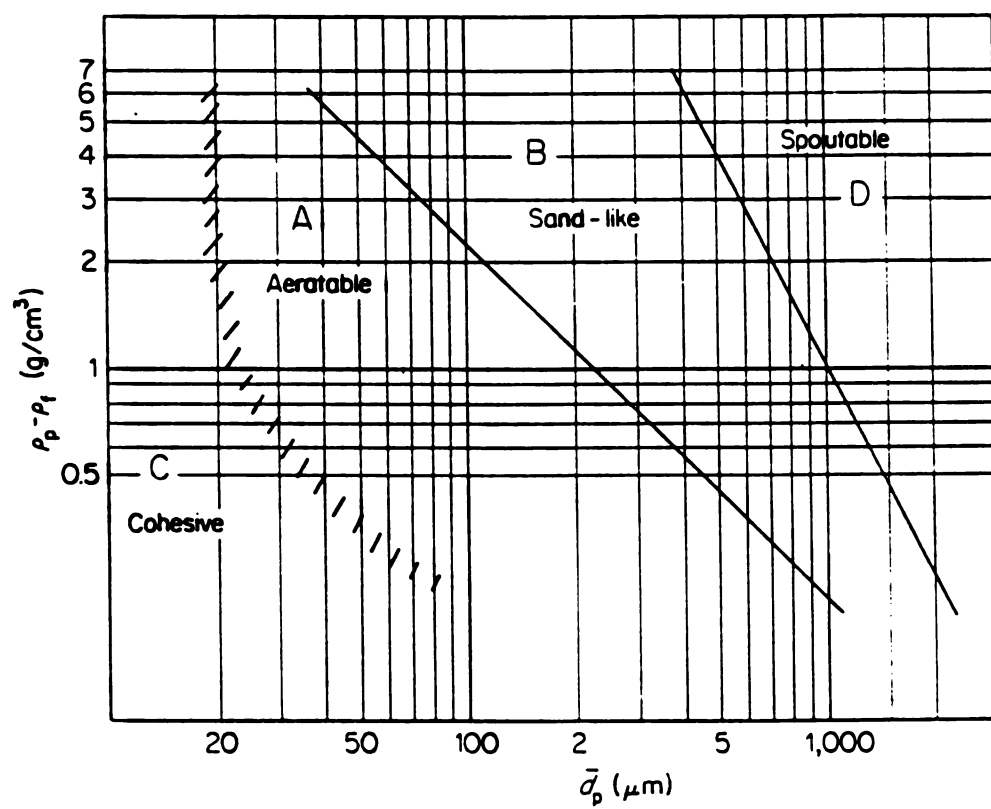


Figure 2.1 Classification of Powders based on Fluidization Behavior ^[18]

2.2.2 Tribocharging

Aerosolization of powders results in frequent contact of the particles with surfaces resulting in the generation of static charges, referred to as tribocharging. Gallo and Lama [21] related contact charging to particle relative permittivity ϵ_r and particle size. These two parameters have a significant effect on the work function, which is defined as the minimum energy required to extract the weakest bound electron from a particle surface to infinity. When particles of different work functions are brought into sliding and/or frictional contact tribocharging is invariably involved [22]. The net effect of the relative permittivity and size of the particle indicates that the work function decreases with an increase in particle size and/or with particle permittivity. Therefore, electron transfer from a larger particle to a smaller particle is favorable which results in large particles being positively charged and small particles being negatively charged. The bipolar charging of many powders may be attributed to this mechanism because of the size distribution in a given powder.

Polymeric materials can be arranged in a Triboelectric series depending upon the sign and magnitude of charge acquired on the surface due to contact and or frictional electrification. Gallo and Lama [21]; and Bauch [23] have separately arranged many polymeric materials in a triboelectric series and found a strong correlation between the macroscopic property of relative permittivity and the sign and magnitude of charge of the material (Table 2.1). At the top of the series is polyamide with a relative permittivity of about 4 which charges positively and at the other end is PTFE having a relative permittivity of 2.1 which charges negatively. The sign and magnitude of the charge

Table 2.1 Triboelectric Series of Polymer Materials

Material	Permittivity	Sign of Charge
Polyamide	3 - 6	+ve
PPS	3.9	+ve
Polyurethane	4 - 6	+ve
Epoxy resin	4	+ve
PEEK	3.2	+ve
Epoxy Polyester	3 - 4	+ve
Polyester + TGIC	3 - 4	+ve
PMMA	3 - 3.5	+ve
Polycarbonate	2.9	-ve
Polystyrene	2.6	-ve
Polyethylene	2.2 - 2.7	-ve
PVC	3 - 6	-ve
PTFE	2.1	-ve

becomes decisive as the distance between the two materials increases in the Triboelectric series. In the case of polymers, the electron affinity of the elements or functional groups bound to the carbon atoms and their stereometric arrangement in the macromolecule influence the sign and magnitude of the charge [23].

The magnitude of charge on a particle is strongly dependent on particle size. The surface charge on a spherical particle increases with the square of the diameter while the mass increases with the cube of the diameter. Hence, the charge to mass ratio increases with decrease in particle size. This makes the effect of triboelectrification more pronounced in the case of smaller particles, especially for size ranges under 50 microns.

Once a particle acquires surface charge, the rate at which redistribution proceeds depends on the electrical relaxation time of the particle. Relaxation time is a product of particle resistivity and permittivity [22]. Insulating materials (most polymers are insulating) having resistivity greater than 10^3 ohms have relaxation times of minutes or even hours, which makes them most susceptible to retaining surface charge. The existence of a surface charge on a particle gives rise to an electrostatic field which has a maximum intensity at the particle surface and decays inversely with the square of distance away from the surface. Bailey [22] estimates the break down field strength of air to be 3.0×10^6 V/m which corresponds to a surface charge density of $26.5 \mu\text{C}/\text{m}^2$. Harper[24] has come up with simplified expressions for the maximum particle charge and the charge to mass ratio for a spherical particle of radius 'r' and density ' ρ '.

Total particle charge	$1.03 \times 10^{-4} r^{1.7}$ Coulombs
-----------------------	--

Charge to mass ratio	$(2.45 \times 10^{-5}) / (\rho r^{1.3})$ C/kg
----------------------	---

While extensive literature has been devoted to the explanation of the cohesive behavior of powders in general, not much research has been done with respect to polymer powders. An attempt to understand the behavior of polymer powders during aerosolization is made in this chapter.

2.3 Powders Investigated

Five different size ranges of Polyamide (Nylon12) powders manufactured by ATOCHEM under the trade name of ORGASOL were used in this investigation. ICI's Victrex PEEK was the next candidate chosen for the study. 3M's Scotchlite hollow glass spheres were also chosen in view of the low density of these particles and the perfect spherical nature of these bubbles. The size distributions of the powders were evaluated by a Java Image Analyze and Malvern Size Analyzer. The shape and surface asperities of the particles were examined under JEOL Scanning Electron Microscope. Table 2.2 summarizes the powders investigated.

2.3.1 Particle Size Analysis

Size distributions of the five different polyamide powders were supplied by the manufacturer. The size distribution and the average particle size was determined for Orgasol-2001 UD Nat1 powder by two different methods; i) Malvern Laser Beam Size Analyzer and ii) Java Image Analyzer. Sizes obtained by both the methods came close to the average size of 10.2 μm quoted by the manufacturer (Malvern size analyzer: 11.2 μm and Java image analyzer: 12.1 μm). While measuring the size distribution in the

Malvern Size Analyzer a dilute surfactant was used to make a dispersion of the polymer particles in water. The average size of all Orgasol powders in Table 2.2 is that indicated by the manufacturer. In the case of Victrex PEEK, size distribution was not available from the manufacturer, and the average size was determined to be 94 μm by the Malvern size analyzer and 97 μm by the Image Analyzer. The size distribution for the Glass spheres was measured using the Malvern size analyzer and the average size was 38 μm .

Table 2.2 Powders Investigated

No.	Powder	Commercial name	Av. Size, μm	Density, g/cc
1	Polyamide	Orgasol-2001UD Nat1	5	1.02
2	Polyamide	Orgasol-2001EXD Nat	10	1.02
3	Polyamide	Orgasol-2002 D Nat	20	1.02
4	Polyamide	Orgasol-2002 ES4 Nat	35	1.02
5	Polyamide	Orgasol-2002 ES6 Nat	65	1.02
6	PEEK	ICI's Victrex	96	1.34
7	Glass Spheres	3M's Scotchlite E22/400	38	0.20

2.3.2 Scanning Electron Microscopy

All the powders investigated were observed using a Scanning Electron Microscope to determine the particle shapes, surface asperities, typical size distributions and presence or absence of particle agglomeration. Low magnification micrographs ($< 300\times$) were taken of the particles as a typical population indicating the general shape of the particles and the size distribution. Micrographs at magnifications greater than $500\times$ were taken to resolve a single particle for its surface asperities.

A close look at Figures 2.2 and 2.3 indicate the fractal nature of the polyamide particles. The particle shape and surface asperities did not change with the change in the particle size as it can be seen that a $5\text{ }\mu\text{m}$ particle is similar to a $65\text{ }\mu\text{m}$ particle. The surface asperities of all the polyamide particles are similar, indicating that different size range powders were directly a result of the polymerization process and not subjected to any size reduction techniques. The porous nature of the polyamide particles is also evidenced from the micrographs. However, it may be noted that the $65\text{ }\mu\text{m}$ powder has a sizeable fraction of smaller particles. In the case of PEEK, (Figure 2.4 (a)&(b)) the neat cleavage surfaces of the particles is indicative that this size range was obtained by grinding the granules. During the course of this study, a sample was prepared which had PEEK particles adhered on carbon fiber. Figure 2.4 (c) shows how the particle adhered to the carbon fiber and Figure 2.4 (d) shows a particle in a completely sintered state.

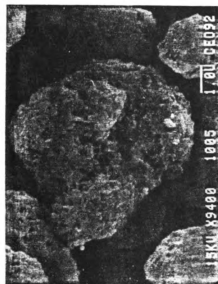
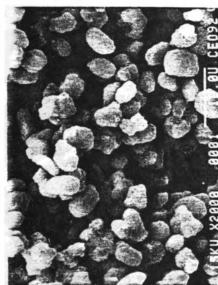
(b) 5 μ Particle(d) 10 μ Particle(a) 5 μ Powder(c) 10 μ Powder

Figure 2.2 SEM Micrographs of Polyamide Powders -Typical Distributions and Surface Characteristics
(5 μ and 10 μ Powders)

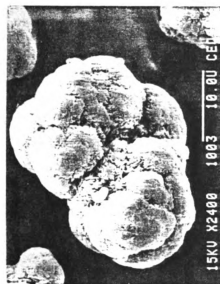
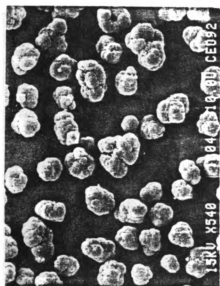
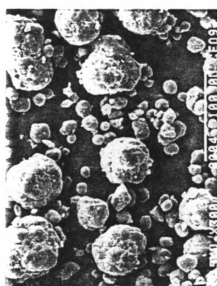
(b) 20 μ Particle(d) 65 μ Particle(a) 20 μ Powder(c) 65 μ Powder

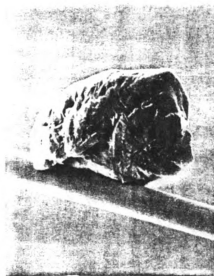
Figure 2.3 SEM Micrographs of Polyamide Powders - Typical Distributions and Surface Characteristics (20 μ and 65 μ Powders)



(a) Powder



(b) Particle



(c) PEEK on Carbon Fiber(Adhered)



(d) PEEK on Carbon Fiber(Sintered)

Figure 2.4 SEM Micrographs of PEEK Powders -Typical Distributions and Surface Characteristics

2.4 Experimental Setup

The experimental setup for providing a vibro-fluidizing condition is as shown in Figure 2.5. A 3 inch ID aerosolizer is used with the vibrating energy provided by a 6.5 inch acoustic speaker. The aerosolizer is a cylindrical plexiglass chamber capped with a rubber diaphragm on the top and bottom. The aerosolizer is charged with powder on to the rubber diaphragm at the bottom, which vibrates with the given frequency and amplitude of the speaker. A sinusoidal wave input is given to the speaker by a B&K function generator which is amplified by a Crown amplifier. Inlet ports for dry nitrogen gas are provided both at the bottom and at the top of the aerosolizer. Near the top of the aerosolizer a disposable filter is connected for determination of entrainment rates.

First, the resonant frequency of the aerosolizer was determined after loading with each of the different powders. To study the effect of a parameter, a set of experiments was conducted at the resonant frequency of the material keeping the amplitude constant. The height to which the powder bed expanded at a given frequency and amplitude is termed bed height. Bed height and the entrainment rate of aerosol in a one hour run period were the criteria used to characterize aerosolization.

The behavior of the cohesive powders with respect to the geometry of the aerosolizer was also investigated. Two aerosolizers were chosen for the study which differed widely in the L/D ratios i) the 3" ID aerosolizer with a L/D ratio of 3.5 (small aerosolizer) and ii) 17.75" ID with a L/D ratio of 1.35 (big aerosolizer). The bed weights were determined by keeping the weight per unit area of the bed constant. Three

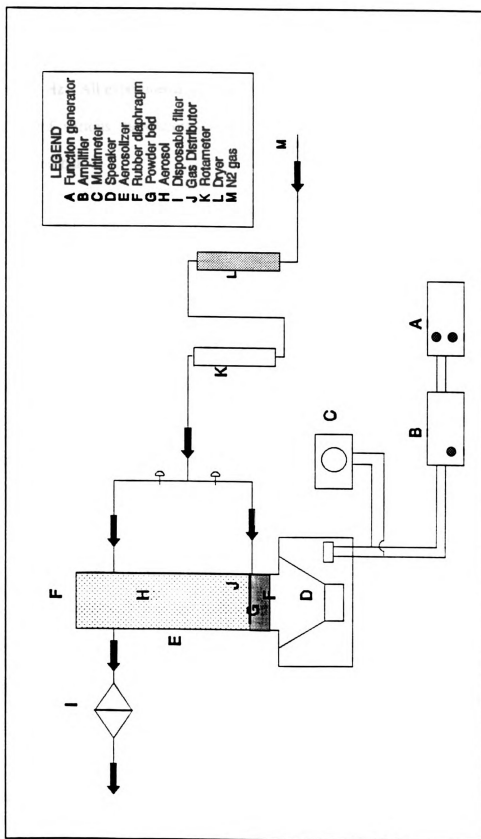


Figure 2.5 Experimental Setup to Determine Aerosolization Characteristics

different levels of weight/area were chosen. The frequency of operation varied from 0 to 30 Hz. All experiments were conducted with the same amplitude of 10.5 V. The effect of various parameters on the aerosolization behavior of these powders are discussed below.

2.5 Results and Discussion

The objective of the aerosolization studies in the small scale setup was to analyze the behavior of aerosolization under various conditions which would help in designing and operating a larger system. Seven powders differing in size, density and shape were used in these studies (Table 2.2). The effect of amplitude and frequency, bed weight, density of powder, size distribution of powder, and gas flowrate on aerosolization was studied.

2.5.1 Momentum Balance

A simple momentum balance around a control volume in the aerosolizer chamber gives an understanding of the various forces at play (Figure 2.6). In equation (1) the upward force on the particles is balanced by the hydrodynamic forces, acoustic forces, shear forces and gravity [25].

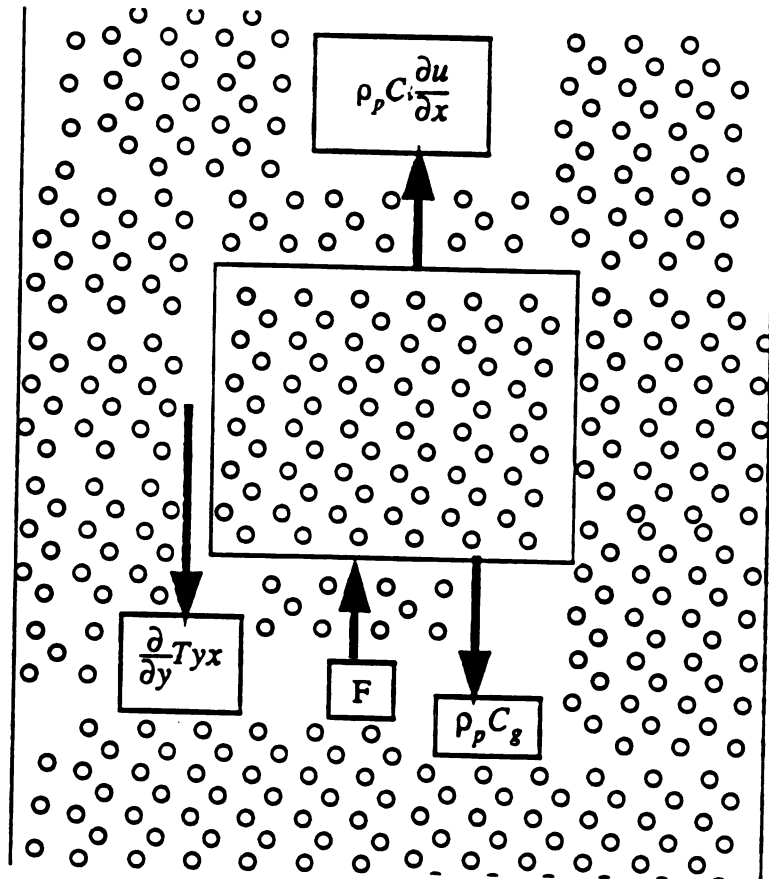


Figure 2.6 Momentum Balance in Aerosolization Chamber ^[4]

$$\rho_p C \frac{du}{dx} = - \frac{dT_{yx}}{dy} - \rho_p g C + F_a + F_h + F_c \quad (1)$$

where,

- ρ_p = particle density
- C = Volumetric concentration of particles
- u = velocity of particle
- T_{yx} = Shear stress
- g = Acceleration due to gravity
- F_a = Acoustic force
- F_h = Hydrodynamic force
- F_c = Inter-particle cohesive forces

Ideally, a mathematical model based on the momentum balance describing the phenomenon of aerosolization would have predicted the design parameters for the scale up. However, the cohesive nature of the polymer powders in the size range of interest and the lack of sufficient literature to predict inter-particle cohesive forces resulted in seeking empirical trends for analyzing the phenomenon of aerosolization by acoustic energy.

2.5.2 Amplitude and Frequency

The effect of amplitude on the aerosolization for 10 μm polyamide powder has been studied by Iyer[4]. In this study the effect of aerosolization height with frequency at constant amplitude was recorded for each of the powder tested. It may be concluded that operation of the aerosolizer at the resonant frequency has a far greater effect on the aerosol height than changing the amplitude. Another investigation led to the conclusion

that vibration of the lower diaphragm and the upper diaphragm is almost in unison implying that the motion of the medium inside the aerosolizer is plug flow. This was confirmed by a vibration detector. An eddy current probe was placed close to the top vibrating rubber diaphragm and the frequency signal read out from an oscilloscope was compared with the frequency counter of the speaker. Despite noise in the oscilloscope read out, peaks matched those of the speaker's frequency.

2.5.3 Bed Weight

The resonant frequency of the aerosolizer does not change in any significant manner with change in bed weight. Three different bed weights of 3.0, 7.1 and 14.2 grams were used in the case of the small aerosolizer and two different bed weights of 250 and 500 grams in the big aerosolizer. Figure 2.7(a) shows this effect for glass spheres in the small aerosolizer and Figure 2.7(b) shows the effect with respect to 5 μ m polyamide powder in the big aerosolizer.

From this experiment, it is concluded that the system should be operated at the resonant or the natural frequency of the acoustic system. Maximum energy is transferred to the diaphragm at the natural frequency irrespective of the powder bed weight. The rubber diaphragm behaves like an elastic spring with the powder bed weight being the dead weight. An increase in the bed weight can be considered as an increase in the dead weight of the spring, with the spring constant remaining the same. Thus, it may be concluded that during a normal run of the process the decrease in the bed weight due to

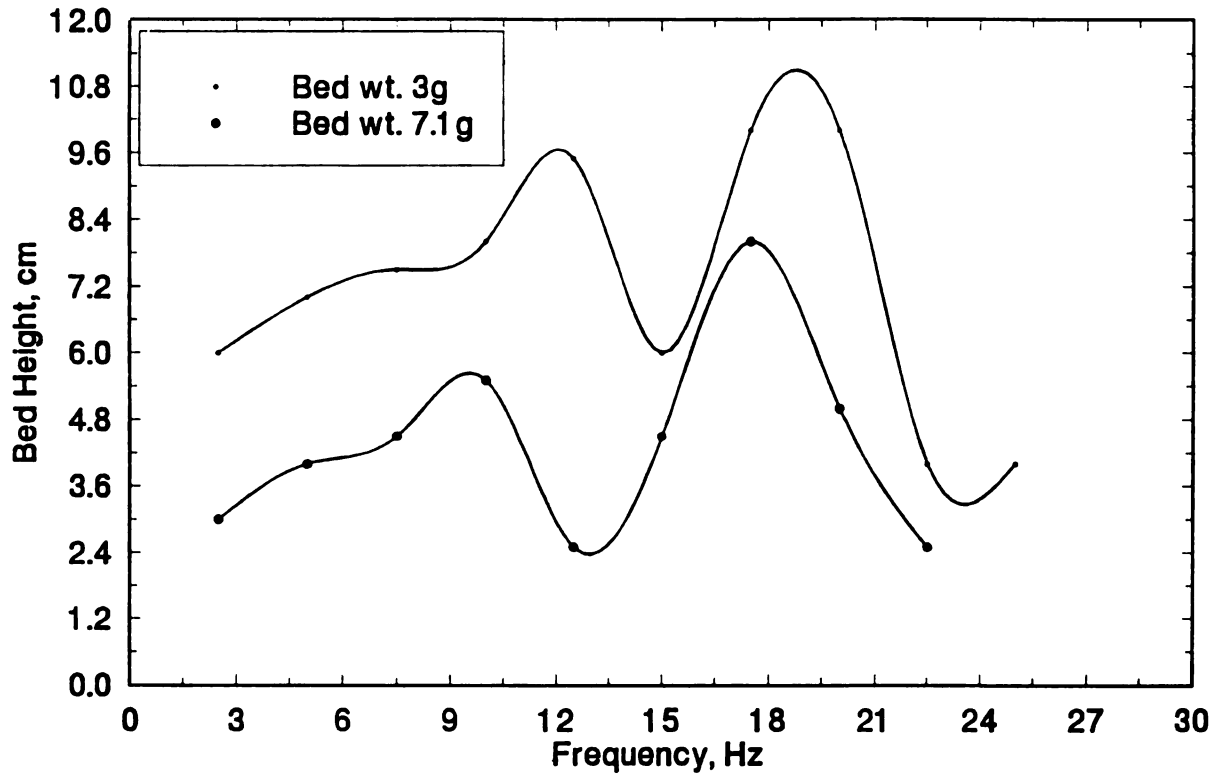


Figure 2.7a Effect of Bed Weight on the Resonant Frequency of Small Aerosolizer (Glass Spheres)

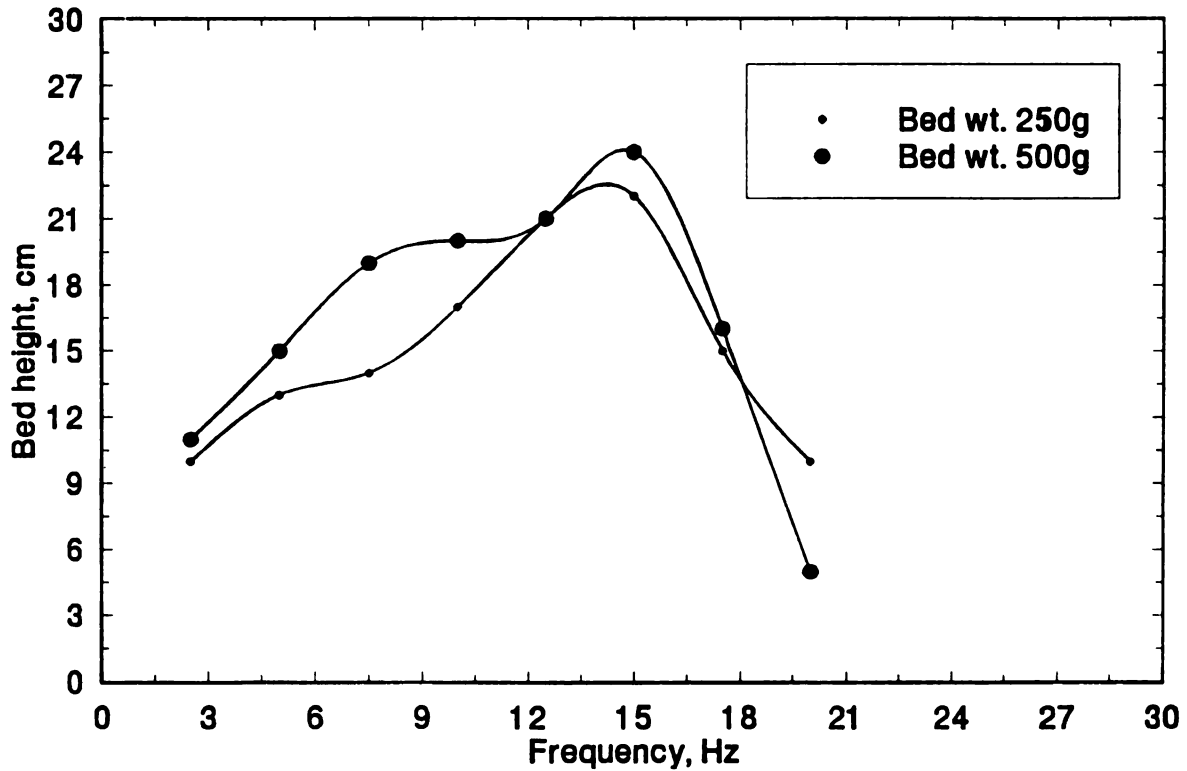


Figure 2.7b Effect of Bed Weight on the Resonant Frequency of Big Aerosolizer (Polyamide 5 μm Powder)

depletion of powder is not going to significantly change the resonant frequency of operation.

2.5.4 Density

The difference in the densities of glass spheres (0.2 g/cc) and 35 μm polyamide (1.02 g/cc) is substantial but are nearly of the same size. However, it is interesting to note that the height to which they aerosolize is nearly the same in a particular aerosolizer setup. This indicates the dominance of hydrodynamic forces over gravity forces.

2.5.5 Gas flowrate

The role of gas flow in the process of aerosolization had to be investigated in terms entrainment of particles out of the aerosolizer through an opening. This gave a comparison between the rate of entrainment due to acoustic energy alone and a combination of acoustic energy and gas flow. Dry nitrogen gas was supplied through an entry port just above the feed bed. The relative humidity was also noted using a sling type RH meter. All experiments were conducted at relative humidity levels of below 50 %. The mass flow rate of particles exiting from the aerosolizer was determined by collecting the particles in a disposable filter for two half hour runs. The average mass flow rate of the two half hour runs were used for further analysis of data. It was observed that acoustic energy alone was not sufficient to entrain the particles out of the aerosolizing chamber in any significant way when operated at the resonant frequency and an energy level of 10 V (Figure 2.8).

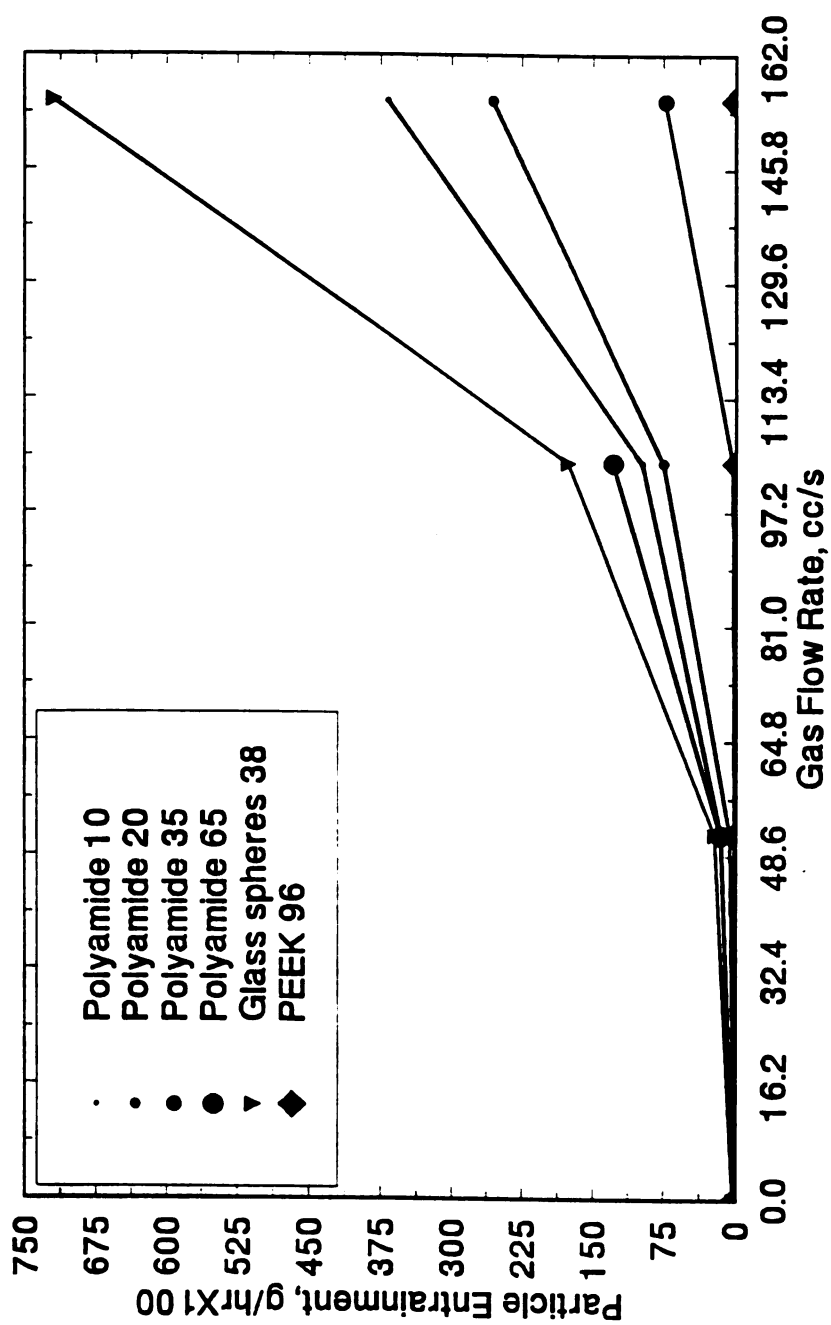


Figure 2.8 Variation of Particle Entrainment with Gas Flow Rate

Gas was supplied at the bottom of the aerosolizer at a rate of 51.6, 104.3 and 155.6 cc/s metered through a rotameter. The particle entrainment rate increases exponentially with gas flowrate as shown in Figure 2.8. Of the three different materials studied only PEEK could not be entrained even at a gas flowrate of 155.6 cc/s while all sizes of polyamide and glass spheres did respond even at lower gas flowrates. This may be attributed to higher density and larger particle size of the PEEK powder. On the other hand glass sphere entrainment is the highest because of their low density.

2.5.5.1 Gas Distributor Ring

The dry nitrogen gas provided a good method for the entrainment of particles. However, preliminary calculations for the operation of the scaled-up aerosolizer indicated the requirement of large gas flows rates, if nitrogen were to be just passed into the aerosolizer from the chamber wall. This led to the development of an efficient gas distributor located just above the aerosolizer powder to impart momentum to the particles and aid in the entrainment [26]. This gas distributor is a tubular ring with small holes drilled at regular intervals on one side of it which would provide vertical jets and is placed in the center of the aerosolizer just above the feed bed (Figure 2.9). This distributor proved to be a very effective means for particle entrainment. For the same gas flowrate the use of the distributor increased the entrainment rate by more than ten times for all the three different materials tested. For a given gas flowrate of 51.6 cc/s comparison of particle entrainment with and without the gas distributor is shown in Figure 2.10 for Polyamide powders of sizes 10, 20, 35 and 65 microns. In all the cases

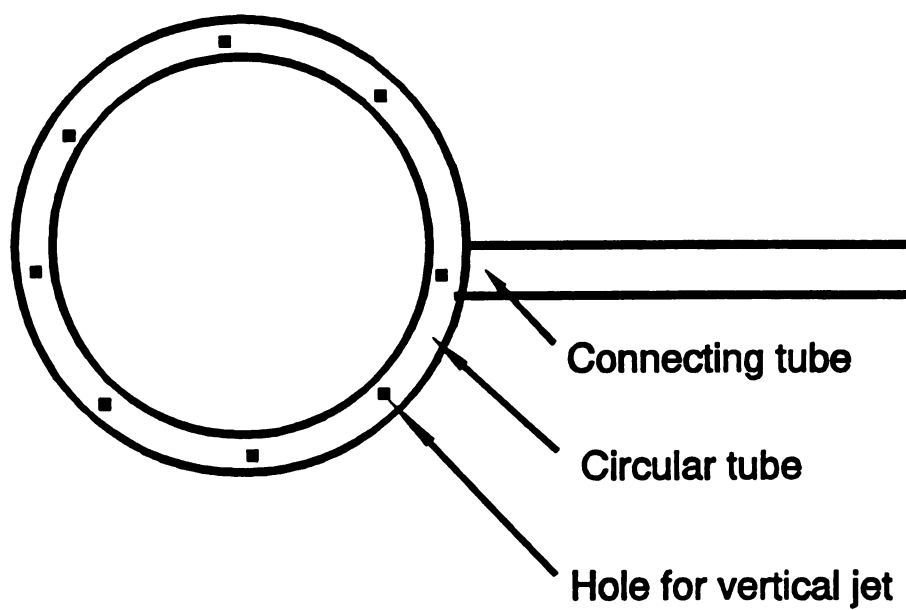


Figure 2.9 Gas Distributor Ring

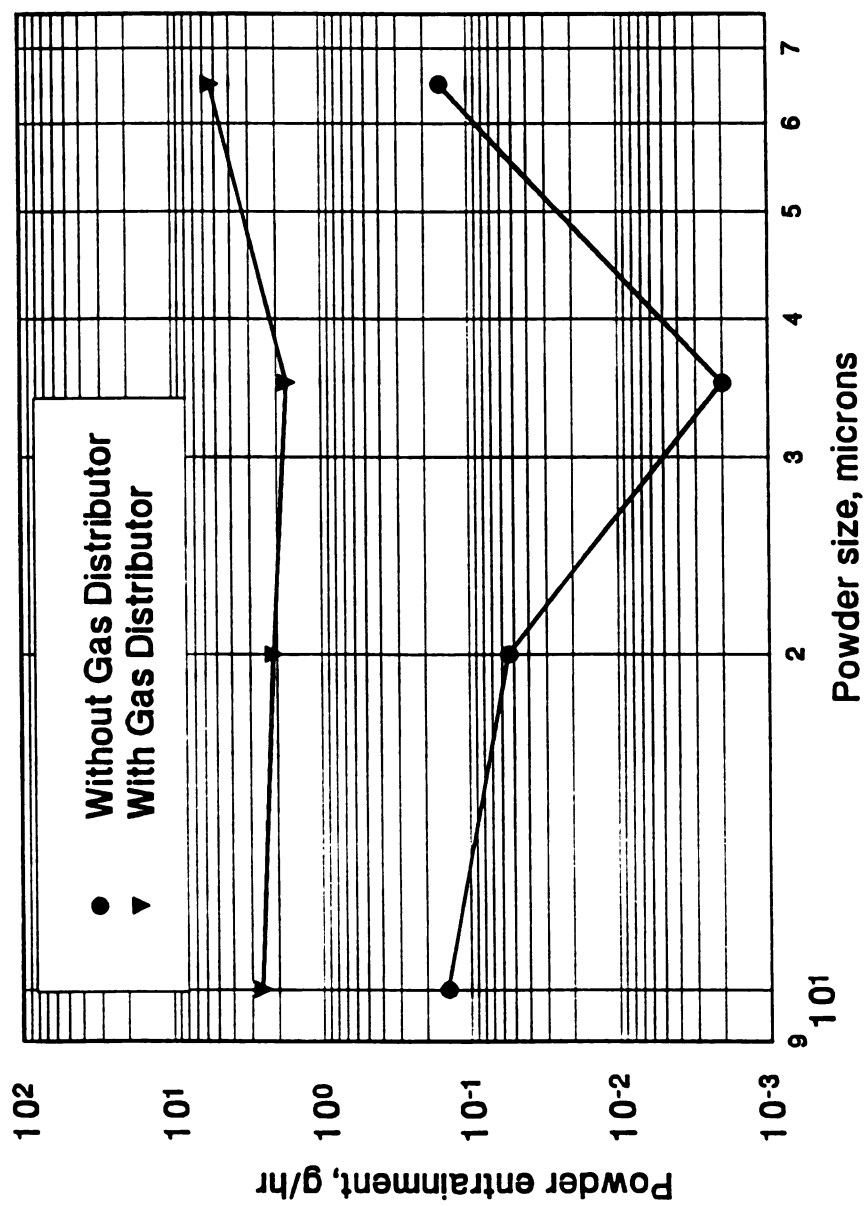


Figure 2.10 Effect of Gas Distributor on Particle Entrainment

there is at least an order of magnitude increase in the entrainment rate after installing the gas distributor.

2.5.6 Aerosolizer size effects

Differences in the behavior of the powders have been observed when aerosolization takes place in aerosolizers with different L/D ratios.

- (i) There is a marked difference in the height to which the aerosol bed rises between the two aerosolizers. The aerosol height is about 10 - 20 cm in the case of the larger unit and 3 - 8 cm in the smaller one irrespective of the powder type for the frequency range studied.
- (ii) The agglomeration of 5 micron particles was significantly less in the case of the big aerosolizer. This may be due to the reduction in the wall effects which accentuate 'balling'.
- (iii) For the operating range of the frequency (0 - 30 Hz) there is only one resonant peak in the big aerosolizer while there are distinctly two peaks in the small one. This is also irrespective of the powder type.
- (iv) Glass spheres with about one fifth the bulk density of nylon still aerosolize to about the same height as nylon particles. This clearly indicates that the drag and buoyancy forces are more predominant than the gravitational forces.

2.6 Summary

From the powder entrainment studies (Figure 2.8 and 2.10), it has been observed that an increase in particle size from 10 to 35 microns follows an expected decreasing trend in entrainment. However, there is a reversal in the trend for the 65 micron powder and there is a dramatic increase in the entrainment rate primarily due to the aeratable nature of the powder. This indicates that while 5 and 10 micron powders are type C powders, the behavior of 65 micron powder alludes to a type A powder and the others lie in-between (type AC). The effect of various parameters on aerosolization characteristics of polymer powders provided the guidelines for designing the scale up aerosolizer.

Chapter 3

Process Design

3.1 Introduction

The successful performance of the prototype powder prepreg process required a technical and economic analysis to determine the prepregging speed for an industrial scale operation. The study conducted by Ball et. al. [17] indicated that for this process to be viable the prepregging speed should be at least 20 cm/s (Figure 3.1) in order to keep the non-material costs around \$1 per pound (based on an annual production of 25,000 pounds). A scaled up version of the powder prepreg process was required to demonstrate the feasibility of operating the process at speeds greater than 20 cm/s. An impregnating system had to be designed for this speed of operation. Analysis of the mode of powder impregnation in the prototype and investigation of the aerosolization behavior of polymer powders (Chapter 2) gave the necessary background to design the impregnating system for the scaled up unit. In this chapter the development of the high speed process is discussed and the design features of each of the units is detailed.

3.2 Process Design Criteria

Based on the economic study and the operational experience gained from the prototype the design criteria for the scaled up powder prepreg process were established.

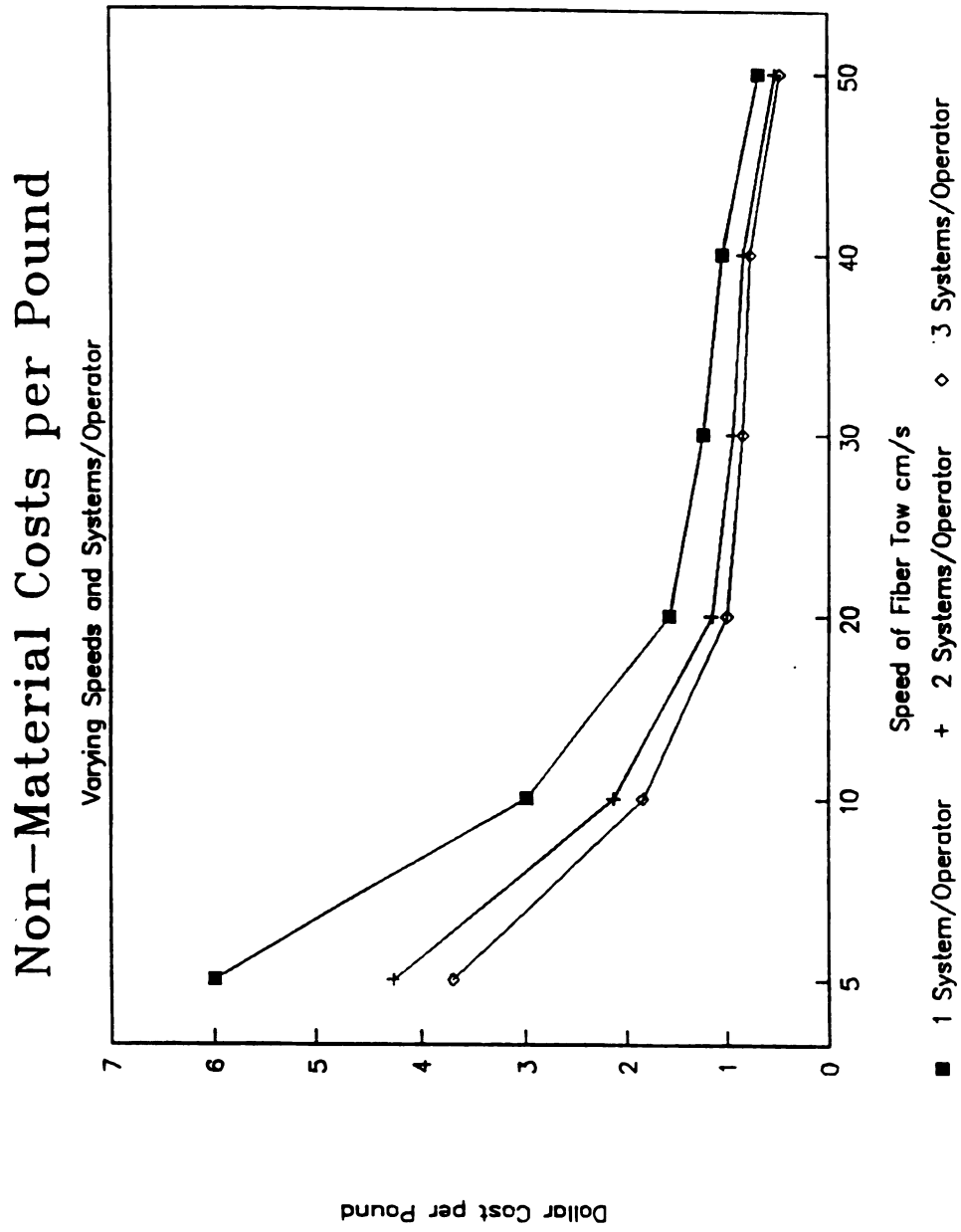


Figure 3.1 Economic Analysis of Powder Process

- i) The prepregging rate of the scaled up version should be at least 20 cm/s with the capability of consistently impregnating any desired polymer to any matrix volume fraction.
- ii) In order to maximize production, the scaled up version should be capable of spreading and impregnating 12K fiber tows.
- iii) A fiber motion system should be designed which incorporates a tension controller to minimize fluctuations in the motion and provides zero tension on the fiber tow in the spreader unit of the process.
- iv) Sintering operation should be capable of sintering the particles on the fibers at the highest rates of prepregging.
- v) A dedicated process control and data logging system should be incorporated for minimum supervision.

3.3 Development of Process Scheme

There are principally four unit operations in this powder process. The operations in sequence are i) spreading the fiber tow; ii) generating an aerosol of polymer powder; iii) impregnating the polymer particles onto spread fibers; and iv) sintering the particles in place. In the prototype, operations (ii) and (iii) were performed in a single stage known as the aerosolizer. It was designed for a line speed of 2 cm/s and each stage of operation was sequenced in a horizontal configuration. In order to maintain the same residence time for the fiber tow in the aerosol at speeds greater than 20 cm/s, the scaled up process would require a horizontal aerosolizer with dimensions nearly 7 feet long in

the direction of fiber travel. The mode of aerosol generation in such a situation can be accomplished either by a large acoustic horn or by using a series of small acoustic speakers. The design of such an impregnating system is subject to operational difficulties and complications in process layout. This led to the concept of separating the operations of aerosol generation and particle impregnation on the fibers. As a result, a separate vertical impregnation chamber coupled with the aerosolizer as an aerosol generator was proposed.

Various design options for an impregnation chamber were considered in terms of design feasibility and operational simplicity. The chamber had to provide an efficient and controllable means for contacting the fiber filaments with the polymer particles. A vertical contact chamber with a counter current contacting means of impregnation was chosen. In this configuration, the entrained aerosol from the aerosol generator enters the top of the impregnation chamber while the spread fiber tow enters from the bottom. The scaled up process was then configured around this impregnating means as shown in the schematic of the process in Figure 3.2.

In the scaled up version of the process, the fiber unwinds from the feed spool and enters the spreader where the tow is spread into individual filaments. The spread fiber tow then passes over a tension sensor roller and enters the impregnation chamber at the bottom. Simultaneously, the aerosol of polymer particles generated by the acoustic means is transported into the impregnation chamber from the top and are deposited onto the fibers. The particles deposited on the fiber filaments are sintered in place in the oven which is positioned above the impregnation chamber. The prepreg tape leaving the oven

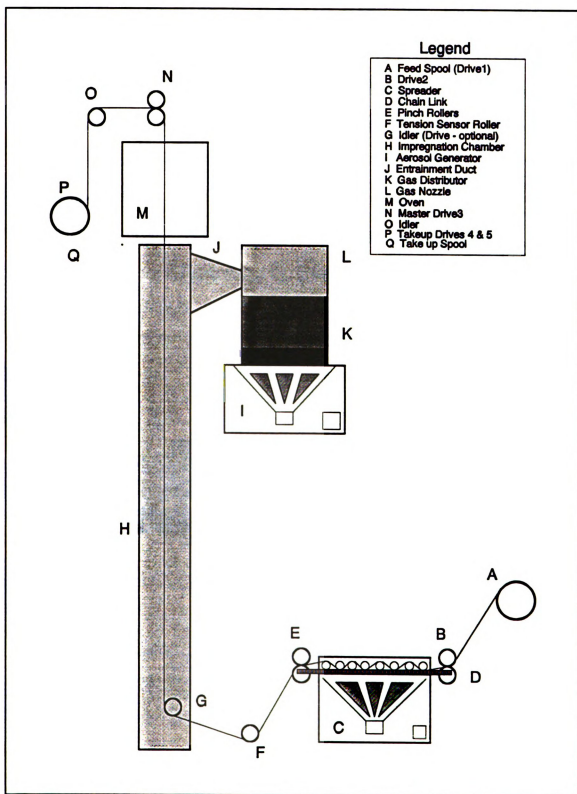


Figure 3.2 Schematic of the High Speed Powder Prepreg Process

is then wound on the take up drum. The fiber tow is driven through the process by a set of five motors controlled by a dedicated motor and tension controller. The fiber motion is discussed in greater detail in Chapter 4 along with other process control aspects. The design of each unit of the process is detailed in the following sections.

3.4 Spreader

The concept and principle of operation of the spreader for the high speed prepregger remains the same as that of the prototype [28]. The design is based on the

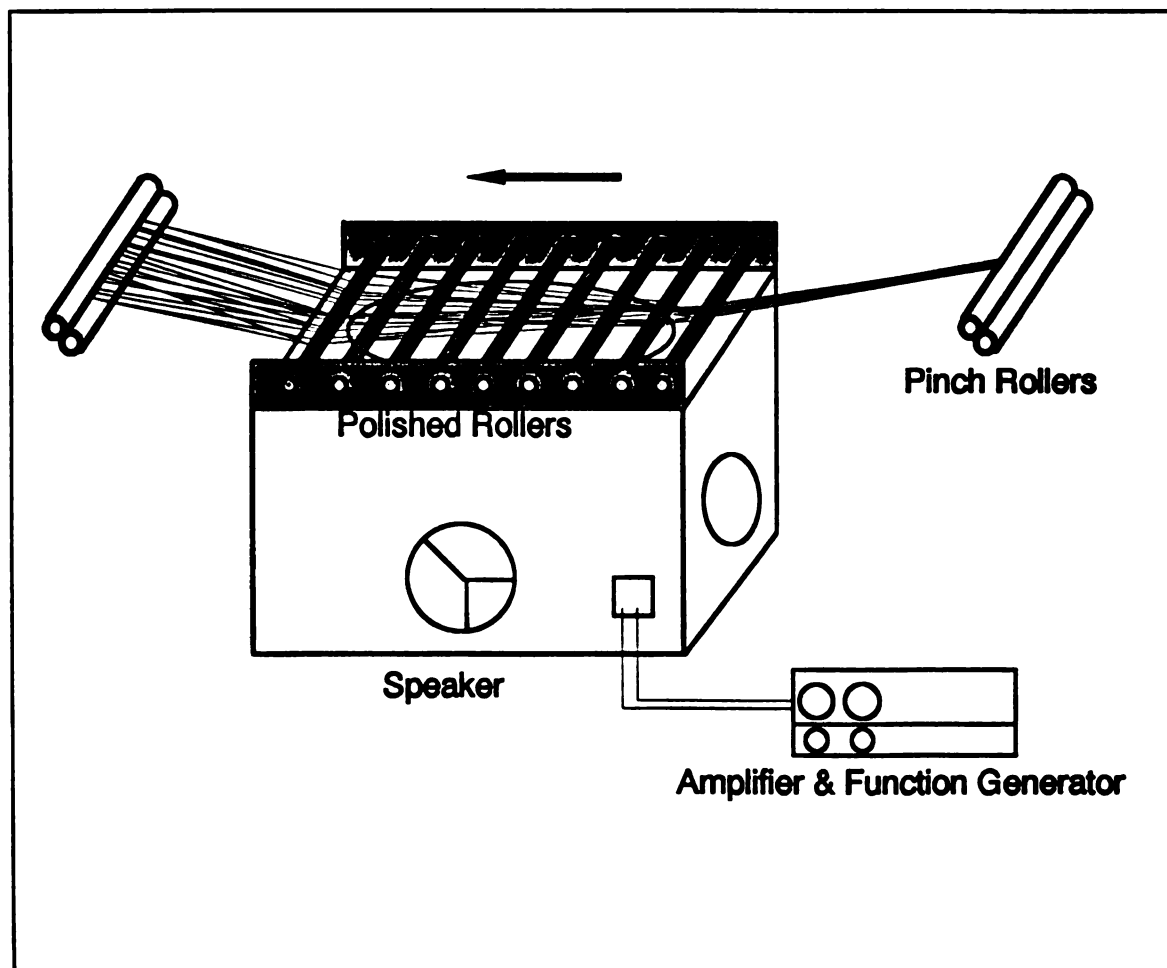


Figure 3.3 Schematic of Spreader

use of pulsating energy provided by an acoustic speaker (Figure 3.3). The speaker vibrates at a constant predetermined frequency and amplitude. The acoustic pressure produced by the speaker is directed upwards and forces the collimated fiber tow to spread out as it passes over a set of polished, friction-free rollers. The function of these rollers is to laterally hold the tow in its spread form (due to friction) while maintaining the forward tow motion. The efficiency of tow spreading is at a maximum when the frequency of operation is at the natural frequency at which the fibers absorb most energy. The fiber tow spread width is also a function of amplitude of the acoustic energy, tension in the tow, and the speed of fiber tow.

The spreader was designed to spread 12K AS4 carbon fiber to expose individual filaments. A 3:1 ratio of speaker size to fiber spread width was used to determine the speaker size. A 15", 100 Watt poly-woofer speaker was selected and a suitable cabinet built around it. On top of the speaker cabinet a set of highly polished case hardened shafts are mounted in friction-less bearings and held in position by an aluminum block mounted on top of the speaker housing and to each side of the speaker.

3.5 Aerosol Generator

In the scaled up process the role of the aerosolizer is now that of an aerosol generator (Figure 3.4). An aerosol of polymer powder which is otherwise difficult to fluidize by conventional fluidization techniques is generated by acoustic means. The principle of operation is similar to that of the prototype aerosolizer developed by Iyer et.al.[28]. A cylindrical plexiglass chamber is charged with a bed of polymer powder.

This chamber has neoprene diaphragms at the bottom and at the top. The powder bed is vibrated and fluidized by the acoustic energy of the speaker operating at a predetermined frequency and amplitude and transmitted to the powder through the diaphragm. In this unit additional buoyancy forces are created by incorporation of a gas distributor and a nozzle which assist in the generation and entrainment of the aerosol.

Acoustic energy coupled with the buoyancy forces of the gases results in entrainment of the aerosol into the impregnation chamber.

The parameters involved in the selection of the speaker size and the dimensions of the cylinder were based on conclusions drawn from experiments conducted on a 3" and 17.75" aerosolizer (Chapter 2). An 18", 200 Watt speaker was selected and a 14.5" ID column with openings for the aerosol entrainment at the top was fabricated. Inlet ports for dry nitrogen gas are provided at the bottom of the column for the gas distributor and at the top for the nozzle. Nitrogen gas is dried and metered using rotameters. Provision for continuously charging the aerosol generator with polymer particles has also been made by incorporating a screw feeder in the system. The screw feeder nozzle is mounted through an airlock in the wall of the plexiglass chamber.

3.5.1 Gas Distributor and Nozzle

A new feature of the aerosol generator is the ability to control the rate of aerosol generation and its rate of entrainment to the impregnation chamber. Dry nitrogen gas is passed into the aerosol generator through a gas distributor located just above the powder bed. This circular gas distributor provides evenly spaced vertical jets of gas

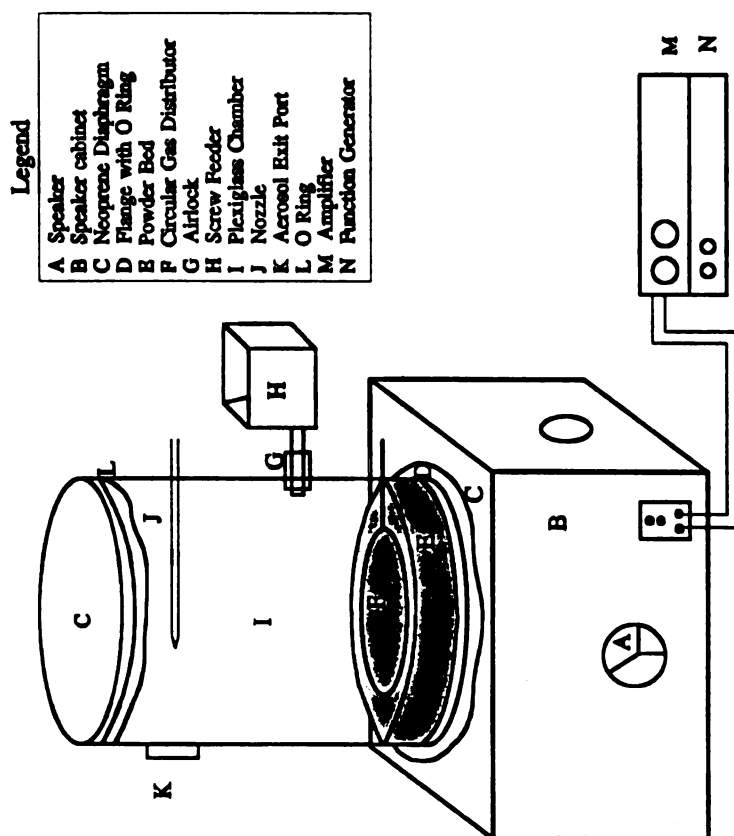


Figure 3.4 Features of Aerosol Generator

(Figure 3.4). Entrainment studies indicated at least a tenfold increase in the rate of aerosol generation and entrainment with the use of gas distributor (Chapter 2). The gas flow momentum of these jets provides upward buoyancy to the particles thereby increasing the rate of aerosol generation. In order to direct the aerosol through the duct connecting the aerosolization chamber and the impregnation chamber, a high speed gas nozzle of dry nitrogen gas was added to the chamber.

3.5.2 Rapping Mechanism

Caking of polymer powder on the aerosol generator walls is a continuous operational problem in the process. Increased caking results in reduced bed weight and lower aerosol generation [4]. In order to overcome this problem, impact type rappers have been installed on the outside walls of the aerosolization chamber similar to the ones installed by Padaki [5] in the prototype process. These rappers are spaced evenly around the plexiglass chamber and an optimum rapping cycle is predetermined for the system.

3.6 Impregnation Chamber

3.6.1 Principle of Operation

A counter current contacting chamber has been designed for impregnating polymer particles onto the spread fiber tow (Figure 3.5) [26,29,25]. This chamber offers flexibility in speed of operation and makes impregnation independent of aerosol generation conditions. It provides the requisite residence time for the powder particles

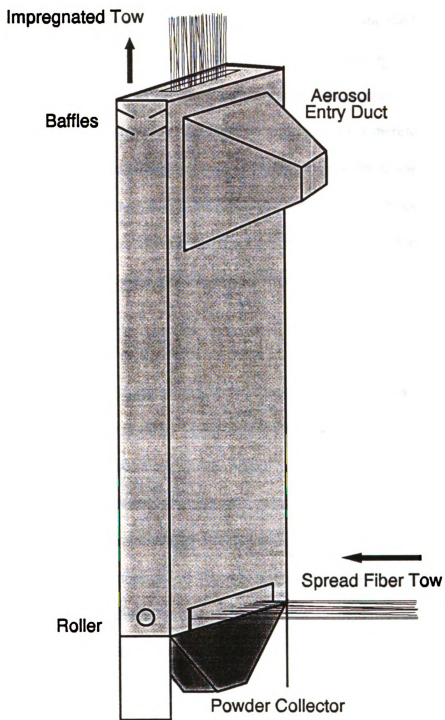


Figure 3.5 Impregnation Chamber

and the fiber filaments to come in contact. The rate of impregnation is directly proportional to the aerosol particle concentration in the chamber and the residence time. The rate of aerosol generation and entrainment can be controlled by either the gas flowrate to the gas distributor or the amplitude of the acoustic energy. The volumetric flowrate of the aerosol entrained into the impregnation chamber is therefore equal to the total gas flowrate used in the aerosol generator. By keeping the amplitude of the speaker constant, the total gas flowrate directly controls the concentration of polymer particles in the impregnation chamber. Thus, at steady state the final volume fraction of matrix on the prepreg tape is a function of line speed and the gas flowrate.

3.6.2 Design Criteria

The underlying principles in designing the impregnation chamber are:

- * Height of the chamber should provide the necessary residence time for the fiber tow to be impregnated. A height of 80" was chosen for a residence time of 10 seconds at the design speed of 20 cm/s.
- * The area of cross section of the chamber should be optimized for the two opposing factors of (a) Particle concentration and (b) Particle settling velocity. It should be noted that an increase in the cross section decreases both the particle concentration for a given gas flowrate and also the particle settling velocity. While a decrease in the particle settling velocity is beneficial for the impregnation process, the decrease in the particle

concentration produces an undesirable effect. The area of cross section chosen was 2"X6".

- * A conical entry duct, rectangular in cross section, is designed which connects the aerosol generator and the impregnation chamber. A sudden expansion in the cross section is provided to create conditions for reducing the velocity of the aerosol that is being transported so that lower particle settling velocities are achieved.
- * The cone angle of the entry duct should be greater than the angle of repose of the powder, so as to avoid a powder build up in the duct due the settling of particles.
- * To minimize the loss of powder and particulate emissions to the surroundings a set of baffles are provided near the top of the chamber.

3.7 Heater

In the heating stage of the process, the particles that adhere electrostatically to the fibers in the impregnation chamber are sintered in place so that handling of the prepreg downstream does not result in loss of powder and that the prepreg acquires the right drape. The heater should provide the necessary residence times for the particles to sinter. The estimated time for heating polyamide-AS4 prepreg tape is 0.012 secs when the particle size is 10 μm [4,30]. A Blue M gravity convection oven was selected which provided a heating zone of nearly 20" thereby a residence time of 2.5 seconds when the line speed is 20 cm/s. The effective heating volume inside the oven was reduced by

sealing the extra space with an insulation panel to improve the thermal efficiency of the oven. The modified oven was positioned in such a way as to heat the impregnated fiber tow moving vertically (Figure 3.6).

The vertical mode of prepreg heating poses certain unique problems. In this configuration, the fact that (i) forced circulation of air inside the oven is not desirable as it might dislodge the particles impregnated on the fibers, and (ii) continuous motion of prepreg requires an entry slot through which cold air also enters, and an exit slot through which hot gases escape by natural convection, makes it extremely difficult to maintain a uniform temperature throughout the heating zone of the oven. Even though the opening for the fiber entry and the exit are as narrow as possible steep thermal gradients are formed inside the oven which result in very short net residence times for the prepreg at the sintering temperature of the matrix desired. The problem of heating is further elaborated while describing temperature control in Chapter 4.

A typical solution to such a heating problem would be to use a tubular furnace with zonal heating, where each zone has an independent temperature controller and all the zonal controllers would coordinate to maintain the desired sintering temperature. Theoretically, one would expect to maintain the desired sintering temperature best with an infinite number of zones.

3.8 Summary

The design of the high speed version involved developing a new vertical scheme for impregnation of polymer particles on the fibers, resulting in the development of the

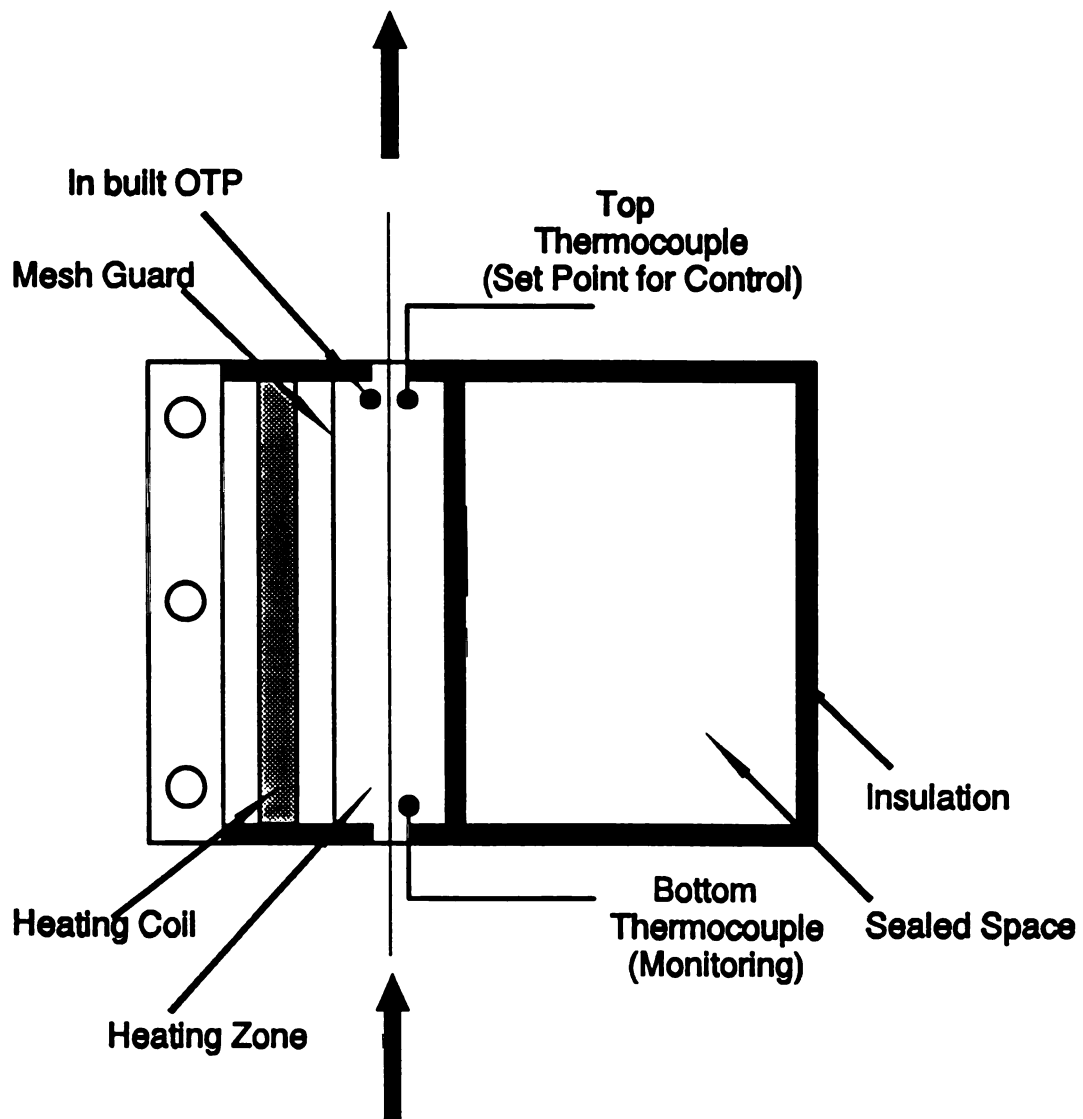


Figure 3.6 Heater For Sintering Operation

impregnation chamber. The principle used in designing the spreader was the same as that used in the prototype process. In view of the vertical configuration, the heater for sintering the prepreg tape requires a more efficient design which takes into consideration the convective currents.

Chapter 4

Process Control

4.1 Introduction

Coupling of the high speed of operation with the brittle nature of the carbon fibers as well as the heating of the impregnated tow in a vertical configuration through the heater are some of the important aspects of this new design which needed careful consideration while designing the control system for this process. In designing the control scheme, the strategy adopted in the prototype [4] was studied and the shortcomings noted by Padaki [5] were taken into consideration. The overall control strategy of this process consists of supervisory control of the system by Dow Chemical's Camile Data Acquisition & Control system [31] and a dedicated Speed and Tension controller (Figure 4.1) [32]. In this chapter, the fiber motion system is discussed followed by the line control strategy and finally the temperature control in the oven. While the various control features are described in this chapter, the performance of the process as a whole is dealt with in Chapter 5.

Camile 2000^R is a data acquisition and control system acquired for this process as part of the effort to automate the process completely. This system will act as the interface between the operator, tension & motor controller system and the process itself.

Camile 2000^R has 8 channel multisensor and analog boards and a 32 channel input/output digital board which operates at 1 Hz. The system is interfaced with all the variables that are to be controlled and monitored. Camile 2000^R forms the supervisory controller of the process.

In view of the slow response time for control action to take place with Camile 2000^R (once every second) a dedicated Speed and Tension Controller had to be designed to overcome fluctuations in the fiber motion. This resulted in controlling the line speed of the process with Camile 2000^R while all the drives are synchronized to run at that speed by the Speed and Tension Controller. Upon a recommendation from Dow, the controller has been custom designed and built by the IDC Corporation. It can control independently all the dc drives as well as take command inputs from Camile 2000^R.

4.2 Fiber Motion

Figure 4.1 shows the path through which the fiber traverses along with the process scheme superimposed with the control strategy. The fiber spool mounted on a cantilever shaft is mounted on a bearing pillow block. The bearing block is fitted with precision ball bearings which makes the shaft rotate freely, however, the shaft is driven by a dc motor (motor1) when the feed spool weighs greater than 4 lbs. Presently, the feed spool is configured to be driven by the motor. The fiber tow then passes through a guide slot and is pulled by the first set of nip rollers.

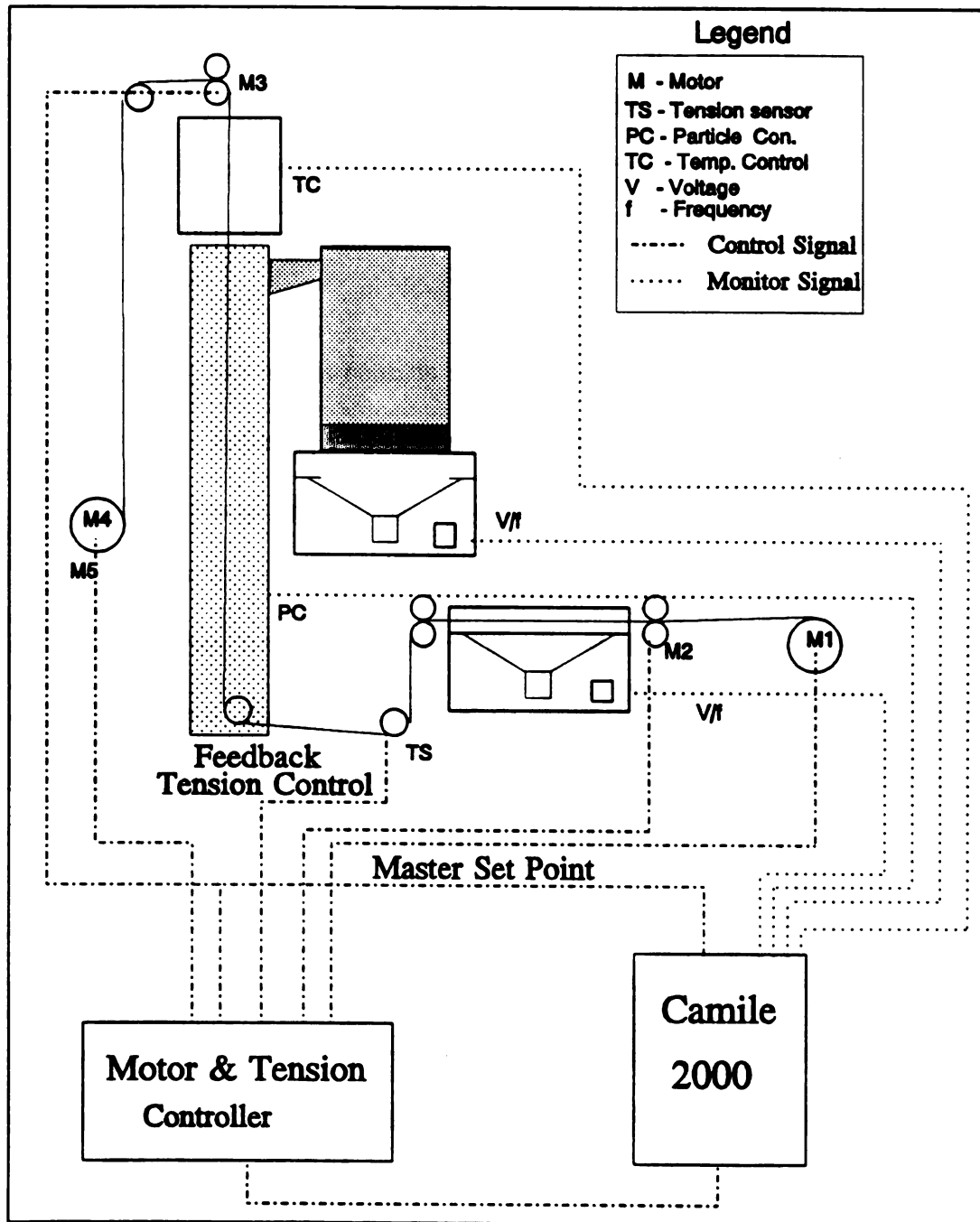


Figure 4.1 Process Control Strategy of the Process

Circular ceramic guides increase the number of twists that would form in the fiber tow especially at higher speeds. It is undesirable to have twists in the tow because they affect the spreading efficiency drastically and subsequently the levels of impregnation. To overcome this, a slotted guide of a cross section 0.04" X 0.75" was designed which ensured that the fiber tow passed through it as a flat tape and minimized the occurrence of twists.

Each set of nip rollers consists of a 1.25" diameter roller (bottom) that is motor driven and a pinch roller of 1" in diameter on the top. All rollers are fabricated from case hardened stainless steel and are mounted on precision ball bearings. The pinch roller, mounted on a precision ball bearing is also free to move in the vertical direction. The fiber tow passes through the spreader and the second set of nip rollers downstream. The bottom shafts of the first and second nip rollers are linked by a chain so that they rotate at the same speed to maintain a net zero tension on the fiber tow in the spreader.

The spread fiber tow goes around a "dancing" tension roller before entering the impregnation chamber. This tension sensor roller is made of a hollow aluminum shaft which is chrome plated and mounted on precision engineered ball bearings fixed in a light aluminum frame which forms one arm of the cantilever frame. The "dancing" motion of the tension sensor roller is caused by the variation in tension in the fiber. The other end of the frame is coupled to two counter weight springs which balance the fiber tension. The objective of the tension sensor is to synchronize the speeds of motors 2 & 3 and also to help in maintaining the spread of the fiber tow entering the impregnation chamber.

The powder on the impregnated fiber tow leaving the impregnation chamber is sintered in the oven located just above it. The fiber is pulled through the impregnation chamber and the oven by a third set of nip rollers driven by motor 3. As it exits the oven, the prepreg tape then passes over an idler roller to change direction before it is finally wound on a take-up spool. The take-up spool driven by motor4 is similar in design to the feed spool and is assembled on a Thomson 2BD Superslide linear motion system. The take up spool winds the prepreg tape across the entire drum as it rasters in a linear fashion. This linear motion is provided by drive5 which reverses direction with the help of two limit switches placed at either end of the linear slide.

4.3 Line Speed Control

A sophisticated line speed control system has been conceptualized for this process which coordinates the operation of five dc motors to provide a line speed ranging from 5 cm/s to greater than 50 cm/s and ensure a constant minimum tension across the spreader. This is achieved by the linking of all the five dc motor controllers to a line speed set by Camile 2000^R with fine tuning provided by motor2 controller with feedback from the tension sensor. Each motor is provided with a dc servo analog PID controller. This PID controller has the unique feature of mixing up to four command inputs to form a composite signal to run the motor. Two command inputs with separate speed and ramp time; a tachometer input with its own scale adjustment; and a fourth input with separate gain and offset can be the inputs to this controller. The command output is a +/- 10 V dc to any power amplifier. The controller provides controlled action in both directions

and can operate in the tach or torque modes. Tuning adjustments of feed forward (K_i), overshoot (K_d) and overall gain (K_p) are provided on the controller. The control features of the five motors of the process have been configured as indicated below.

Motor 1	Tach mode; unidirectional in rotation
Motor 2	Tach mode with command inputs from Tension sensor and master set point of motor3; unidirection in rotation
Motor 3	Tach mode with command input from the Camile; unidirectional in rotation. The speed of this motor sets the line speed of the process.
Motor 4	Tach mode with command input from motor3; unidirectional in rotation
Motor 5	Tach mode with command input from motor3 and limit switches to reverse direction of motion

The performance of this Speed and Tension Controller has been satisfactory and it gives the flexibility of fine tuning the tension at any line speed.

4.3.1 Tension Control

Operation under steady state requires that the speeds of motor 2 and motor 3 be synchronized. A feedback tension control loop incorporated in the process serves this purpose (Figure 4.2). A change in fiber tension due to a disturbance in the fiber motion is reflected by the angular movement of the frame. The position of the frame is monitored by Allen Bradley's absolute optical position encoder [33]. The position

encoder is fine tuned to serve as a feedback signal to control the speed of motor 2 so that it matches the speed of motor 3. The frame tends to come to its equilibrium position due to forces (forces of the counter weight springs) acting in the opposite direction to the tension in the fiber. The output from the encoder is converted to an analog signal and connected to the PID controller of motor 2 to complete the feedback loop.

4.4 Temperature Controller

The heating of the impregnated fiber tow is accomplished in a modified gravity convection oven as described in Section 3.7. Very steep thermal gradients are created in the oven across the entry and exit of the oven due to the rising convective flow of hot air. This can be noted from Figure 4.3 where the temperature profile across the bottom and top of the oven was plotted against time at a set point of 200°C. The situation is aggravated because of the lack of any air circulation inside the oven. This oven is originally fitted with a direct acting thermostat which responds to the oven temperature. The control consisted of a sensing bulb, capillary tube, diaphragm and electrical contacts. The rise in oven temperature expands the fluid in the system forcing the diaphragm outward. The motion of the diaphragm opens or closes a set of electrical contacts which supply power to the heating elements of the oven. This controller also has a separate Over Temperature Protection (OTP), which shuts off the power to the oven if the temperature exceeds a maximum of 25°C over the set point. Due to the location of the sensing bulb near the top of the oven, frequent overheating of the bulb used to occur resulting in the shutting off of the oven. This required a manual restart for the oven.

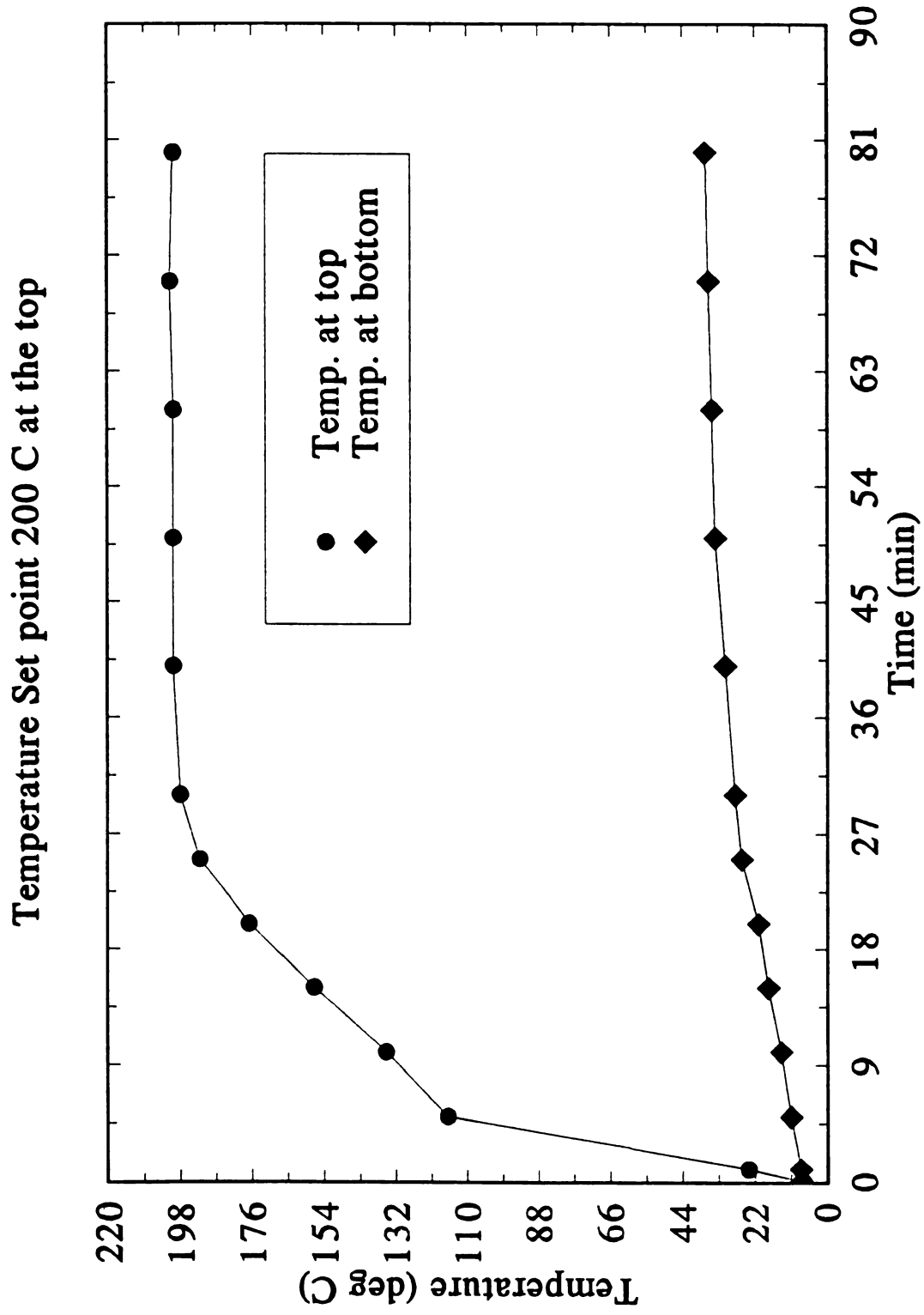


Figure 4.3 Oven Temperature Profile

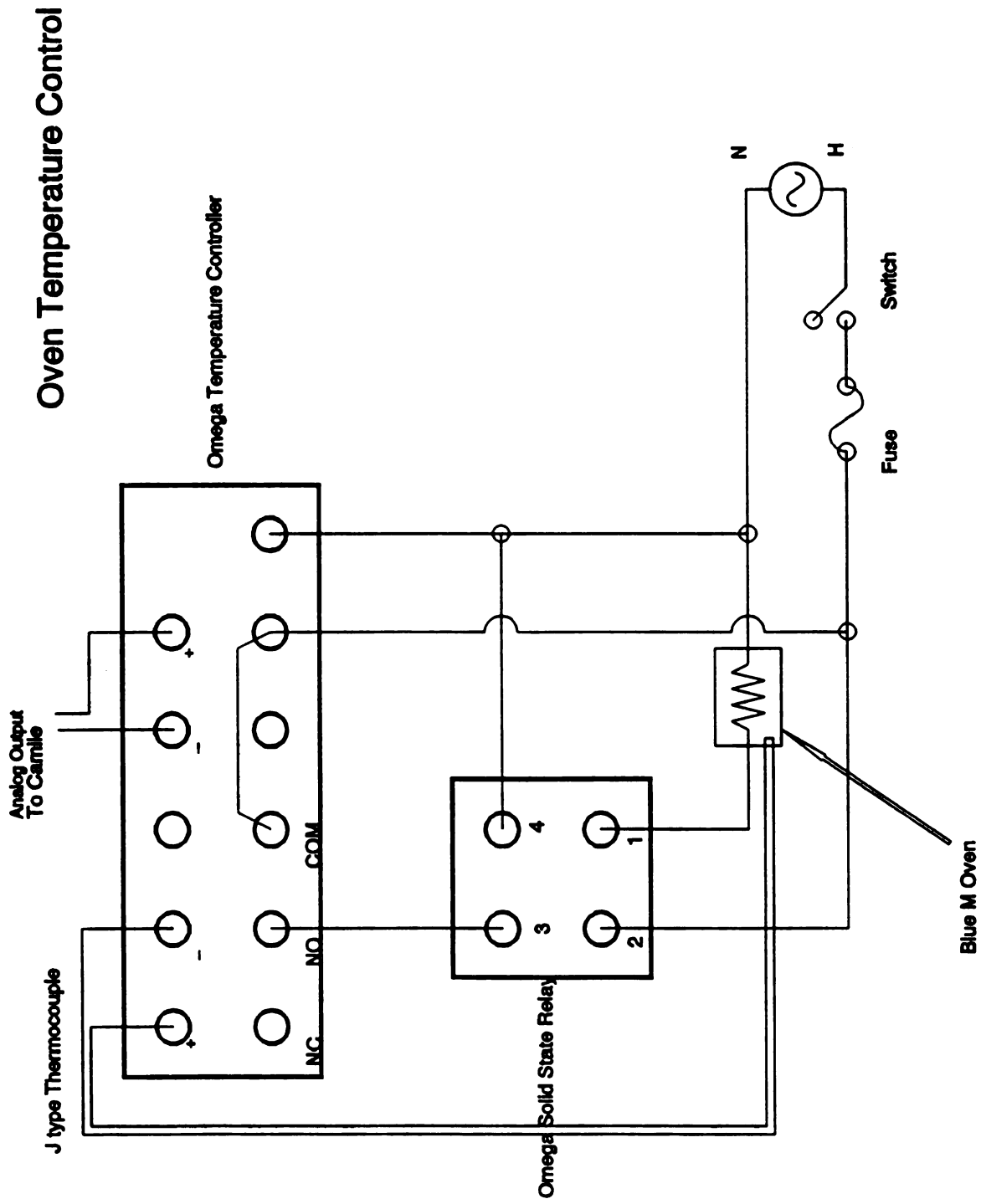


Figure 4.4 Temperature Control Circuit for Oven

An Omega temperature controller with a J type thermocouple as the sensor was incorporated to overcome the difficulties encountered with the existing controller in the oven. The external Omega controller bypasses the controller in the oven but the OTP remains intact. In view of the high amperage of the oven, a solid state relay had to be incorporated in the circuit as indicated in Figure 4.4. The location of the thermocouple is critical in terms of optimum control of the temperature. The thermocouple was placed at the exit of the oven where the temperature is expected to be the highest. With the incorporation of this solid state controller the problem of frequent tripping was eliminated, however, the temperature profile inside the oven has to be monitored to obtain the desired sintering levels in the prepreg tape.

4.5 Process Variables

While the variables related to the fiber motion are controlled by the Tension and Motor controller there are other variables which influence the process. Both acoustic speakers require the voltage (amplitude) and the frequency of operation to be monitored. In the present state of operation both these parameters are set at predetermined values at the start of a run and are monitored by the dual display Fluke 45 multimeter. The frequencies and power levels remain constant and do not require adjustment. The flowrates of the dry nitrogen gas to the gas distributor and the nozzle are also fixed at the start of the run and metered by Cole Parmer rotameters without adjustment.

4.6 Summary

Effective and reliable control forms the key to the success of this process. The line speed control strategy adopted performs well at the high speeds of operation. A better means for heating and controlling the temperature of the prepreg is required. In a manufacturing version of this process, the addition of an on-line feedback system to the control system to monitor and control the impregnation level on the prepreg, would be desirable.

Chapter 5

Prepreg Processing

This chapter describes the high speed processing of prepreg tape. The performance of each unit of the process is evaluated with respect to the design of the process and the performance of the system. The fiber matrix system used for manufacturing the prepreg was AS4 12 K carbon fibers and the polyamide powder matrix. The performance of the process was evaluated in terms of (i) the ability to manufacture prepreg at speeds greater than 20 cm/s; (ii) the ability to impregnate and control to obtain the desired volume fraction of matrix.

5.1 Materials

AS4 carbon fibers from Hercules and Orgasol polyamide powder from Atochem were the materials used to demonstrate the operation of the scaled-up version. In order to compare the performance of the scaled-up version with that of the prototype, the fiber-matrix system has been kept the same. Moreover, the availability of the polyamide powders in different size ranges up to 100 μm with tight distributions has also been a favorable aspect of choosing this matrix. Some of the properties of the polyamide (Orgasol powder) matrix pertinent to the process have been evaluated. The average particle size is determined to be 10.2 μm (Section 2.2). The melt temperature of the

powder, determined using a DSC, is 175°C. The properties of the fiber and matrix important for this process are listed in Table 5.1. All the fiber properties are quoted from the manufacturer's literature.

Table 5.1 Material Properties

AS4 12 K Carbon Fiber		Orgasol 2000 Polyamide Matrix	
Av. diameter, μm	8.0	Av. particle size, μm	10.2
Sp. gravity	1.8	Sp. gravity	1.02
Tensile Strength, Ksi	580	Melt Temperature	175°C
Modulus, Msi	31	Viscosity Pa.s (0.1 sec ⁻¹ 197.3°C)	52.6
Specific heat cal/gm/°C @ 175°C	0.27	Specific heat cal/gm/°C @ 140°C	0.81±0.16
Thermal conductivity W/m/°C	5.73	Thermal conductivity W/m/°C	0.22 - 0.31

5.2 Spreader Performance

The width of the spread fiber tow under normal operating conditions depends on the (i) amplitude of the acoustic speaker at the natural frequency; (ii) speed of fiber tow; and (iii) tension in the fiber tow. A series of experiments were conducted to determine

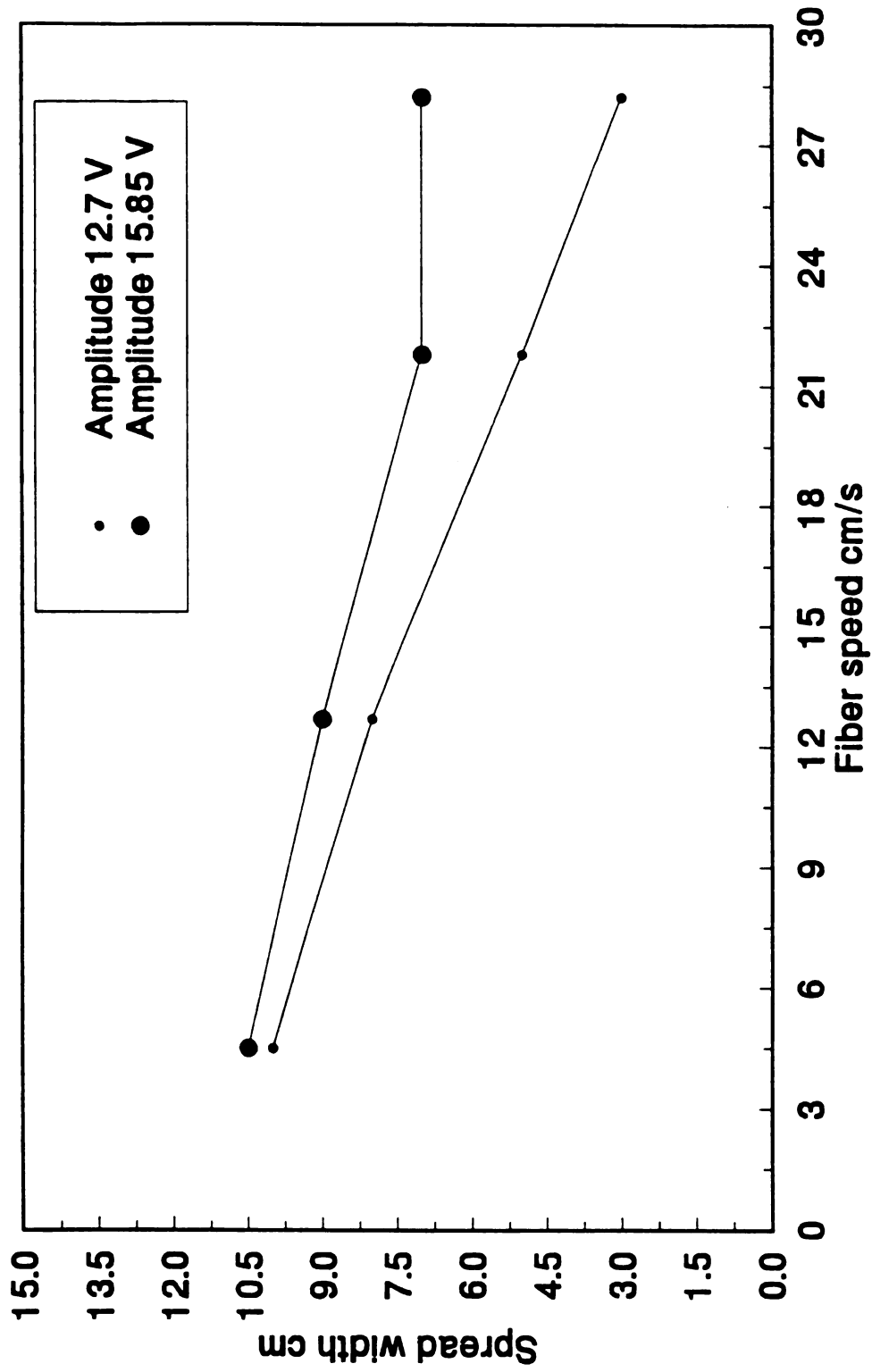


Figure 5.1 Effect of Speed and Amplitude on Spreading

the natural frequency of the unit. The natural frequency band at which the spread width is maximum at a given amplitude is found to be 15.5 - 16.0 Hz for the system.

An experiment was conducted to determine the effect of fiber velocity on spread width (measured at the exit of the spreader). The spreader was operated at two different amplitude levels of 10 V and 15 V. The spread width was noted as the speed of the fiber tow was increased to 30 cm/s (Figure 5.1). As expected the spread width decreases with an increase in speed, however, when operated at a higher amplitude the rate of decrease of the spread width is drastically reduced and the spread width is almost independent of the speed. This may be attributed to the fact that spreading is a direct function of amplitude or acoustic energy and at higher speeds less energy is transmitted to the fiber tow compared to lower speeds resulting in smaller spread widths. While at higher amplitudes, the rate at which energy is transmitted to the fibers is so high that the effect of tow speed is not the dominant factor.

5.3 Aerosol Generation

The system parameters that are needed to establish the processing condition for aerosol generation are (i) determining the natural frequency of the aerosol generator; (ii) optimizing the gas flowrates to the gas distributor and the nozzle to get the desired aerosol entrainment into the impregnation chamber; and (iii) determination of the conditions necessary for the aerosol generator to run the process at steady state.

The effect of bed weight on the natural frequency of the generator was ascertained by charging the chamber with different bed weights - 250, 500, 750 and 1000 grams and

observing the frequency at which the maximum displacement of the powder bed occurs. As explained earlier natural frequency is independent of bed weight.

5.3.1 Gas Flowrates

Dried nitrogen gas is supplied separately to the gas distributor ring and the nozzle at predetermined flowrates. The gas distributor ring located just above the powder bed provides an upward thrust to the particles which are expanded as aerosols due to the vibrating diaphragm. The upward thrust provided by the momentum of the vertical gas jets located all along the circular distributor lifts the aerosol of particles upwards. The nozzle placed near the top of the generator directs the aerosol toward and transports it through the opening in the generator wall into the impregnation chamber. The relative significance of the gas distributor and the nozzle in entraining the aerosol and effectively controlling it forms an important criteria in deciding the gas flowrates to each of these implements. Figure 5.2 & 5.3 show the operating curves obtained from a study in which the particle entrainment rate is plotted against the nozzle gas flowrate and the distributor ring gas flowrate. It is evident from these curves that the gas distributor ring makes a larger contribution to the total aerosol transported than the nozzle. This is in agreement with the assumption that the function of the distributor ring is to generate the aerosol of particles while the high speed nozzle helps in directing the aerosol through the duct into the impregnation chamber. As more aerosol is generated, the entrainment can still be controlled by the nozzle.

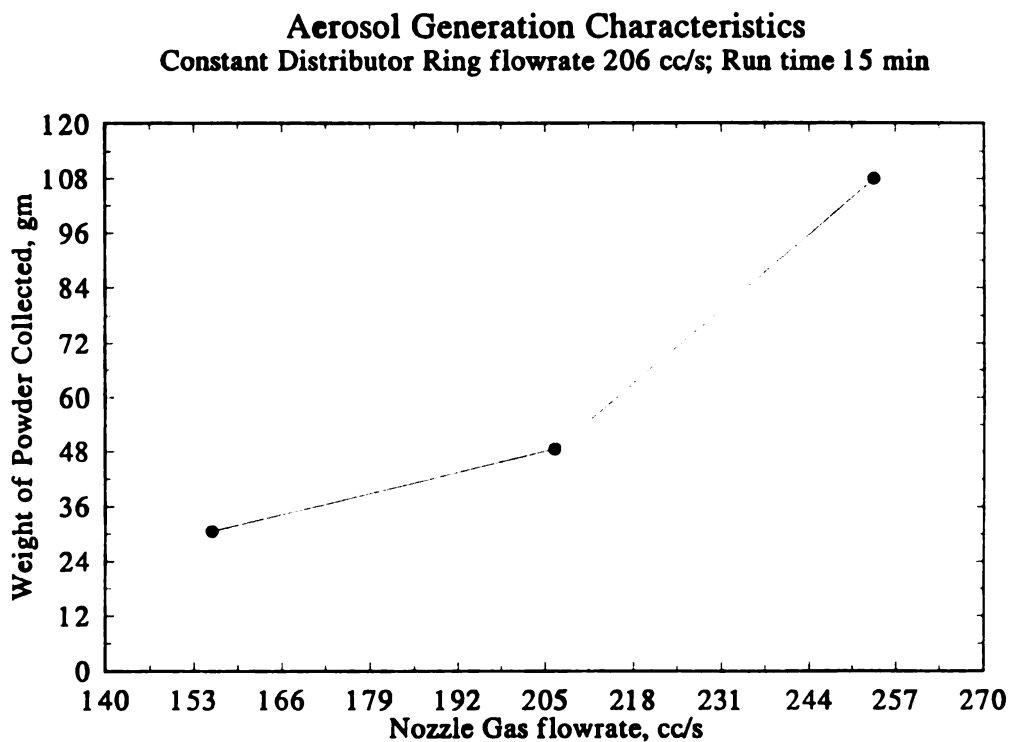


Figure 5.3 Aerosol Generation Characteristics - Constant Distributor Flowrate

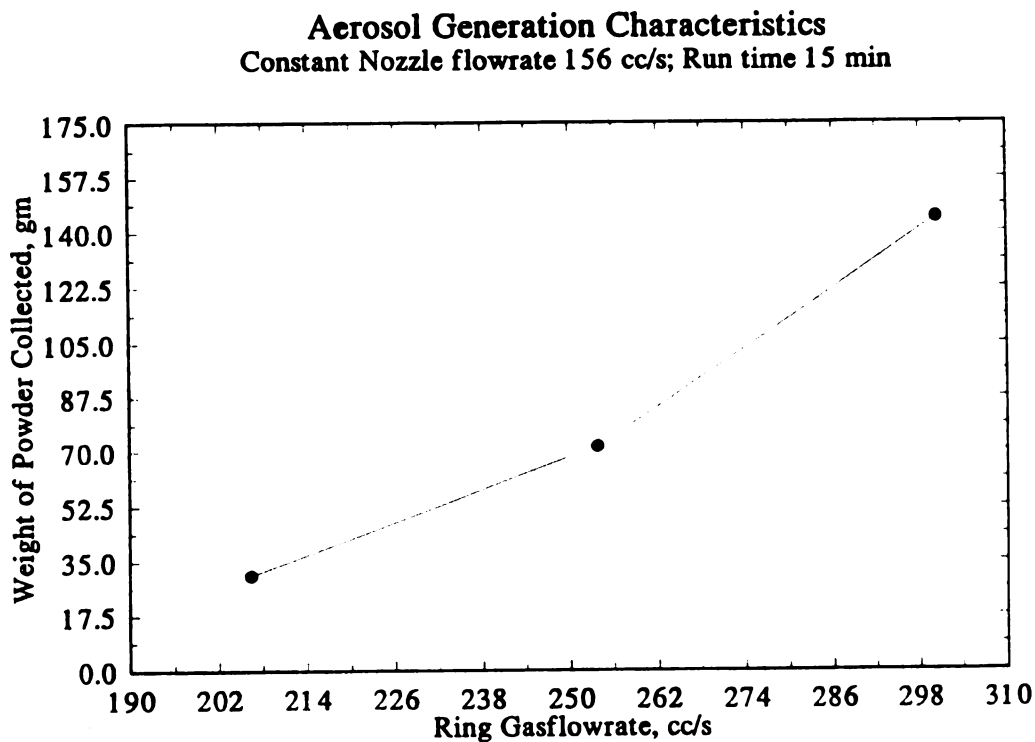


Figure 5.2 Aerosol Generation Characteristics - Constant Nozzle Flowrate

The concentration of particles in the aerosol is a important parameter which controls the rate of powder impregnation on the fibers. The gas flowrate is optimized to get the maximum concentration of particles per unit volume of the aerosol entering the impregnation chamber but at the same time the amount of powder that gets settled at the bottom of the chamber and needs to be recycled is kept to a minimum. The strategy adopted to optimize the gas flowrate was to first fix the gas flowrate to the distributor which generates enough aerosol for the levels of impregnation needed and then control the gas flowrate to the nozzle so that the desired volume fraction of matrix is achieved.

Operation of the aerosol generator for long times depletes the powder in the chamber which reduces the particle concentration in the aerosol entrained. It has been noted that the natural frequency of aerosolization is not affected by the bed weight and which fortunately does not require any continuous changing of the frequency of operation. However, the chamber needs to be charged with fresh powder on a continuous basis. An AccuRate^R screw feeder has been incorporated in the process which has the capability of charging the chamber on a continuous basis.

5.4 Process Runs

The task of demonstrating that the process is capable of operating at speeds greater than 20 cm/s involved continuous refining of the system's hardware to overcome the problems encountered in setting and fine tuning of the operating variables to get the desired prepreg quality. First the fiber speed and tension control system was tested for performance and the speeds calibrated to the dial settings. The scaled-up process has a

capability of controlling the fiber motion from 4.5 cm/s to over 50 cm/s. In view of the near industrial scale of manufacture, operating problems which could have been otherwise overlooked in a laboratory scale of operation needed immediate attention. Eighteen runs, typically lasting 30 minutes each, were conducted on this scaled-up version to fine tune and demonstrate the versatility of the process. Table 5.2 gives an indication of the versatility of the process for the six runs that were conducted when the process was considered stable.

Table 5.2 Summary of High Speed Prepreg Process Runs

Operating Line Speed cm/s	Aerosol Entrainment Rate (Total Gas Flowrate) cc/s	Pick up Vol. Fr. Matrix %	Production Rate, lb/hr
4.5	410	39.87	0.4
21.8	456	21.03	1.6
21.8	460	28.69	1.7
21.8	506	43.31	1.9
21.8	554	43.75	2.0
30.0	554	45.76	2.9

The protocol adopted in running the process was to first set the conditions at which the spreader, aerosol generator and the oven are to operate for the desired line speed and volume fraction of matrix. The process variables which had to be set were the amplitude and frequency of the acoustic speakers of the spreader and the aerosol generator; the gas flowrates to the distributor ring and the nozzle; and the oven

Table 5.3 Typical Analysis of a Process Run

Line Speed - 21.8 cm/s
 Gas flowrate 1- 300 cc/s (Distributor Ring)
 Gas flowrate 2- 156 cc/s (nozzle)

Wt of bare fiber/meter	.80208	gm/m		
Density of carbon fiber	1.8	gm/cc		
Density of Nylon	1.02	gm/cc		
S. No.	Prepreg (wt)	Wt. Fr. Fiber	Vol fr. fiber	Vol fr. m
1	.9158	.8758244	.7998705	.2001295
2	.9835	.8155363	.7147179	.2852821
3	.925	.8671135	.7871264	.2128736
4	.889	.9022272	.8394628	.1605372
5	.9553	.8396106	.7478823	.2521177
6	.889	.9022272	.8394628	.1605372
7	.9226	.8693692	.7904117	.2095883
8	.9102	.8812129	.8078318	.1921682
9	.983	.8159512	.7152803	.2847197
10	.8979	.8932843	.8258869	.1741131
11	.8975	.8936825	.8264876	.1735124
12	.9514	.8430523	.7527127	.2472873
13	.9275	.8647763	.7837333	.2162667
14	.8976	.8935829	.8263374	.1736626
15	.9246	.8674886	.7876721	.2123279
Average	.8683293		.7896584	.2103416
Standard deviation	.0276088		.0397611	.0397611
Wt.fr. of matrix	.1316707			
Vol. fr. of matrix	.2103416			

temperature. Prepreg tape wound on the take up spool was analyzed gravimetrically to determine the volume fraction of the matrix deposited on the fiber. At least ten prepreg samples one meter long, were cut at random from the take-up spool and weighed to determine the average volume fraction of the matrix in the run. The statistical average weight of one meter long bare 12 K fiber tow run through the process has been determined and is used in the calculations to determine the volume fraction of matrix. A typical analysis of a run at 21.8 cm/s is shown in Table 5.3.

5.5 Sintering Operation

The polymer particles are impregnated in the impregnation chamber are sintered in place in the heater in this process. As discussed earlier optimum conditions for sintering have not been achieved in this process in view of the limitations in the oven. A close look at the SEM micrographs in Figure 5.4 (a) and (b) indicates that the particles that have been impregnated are slightly sintered in place. The matrix droplets can be seen in a thermodynamic equilibrium in Figure 5.4 (c), where a prepreg sample (partially sintered by the process) was heated in a hot cell. In the case of the line speed 21.8 cm/s, the particles can be seen starting to sinter while in the case of 30.0 cm/s the particles have undergone less sintering.

5.6 Summary

The versatility of the process lies in (i) the capability of operating the process at a wide range of speeds - as low as 4.5 cm/s to as high as 30 cm/s; and (ii) the volume

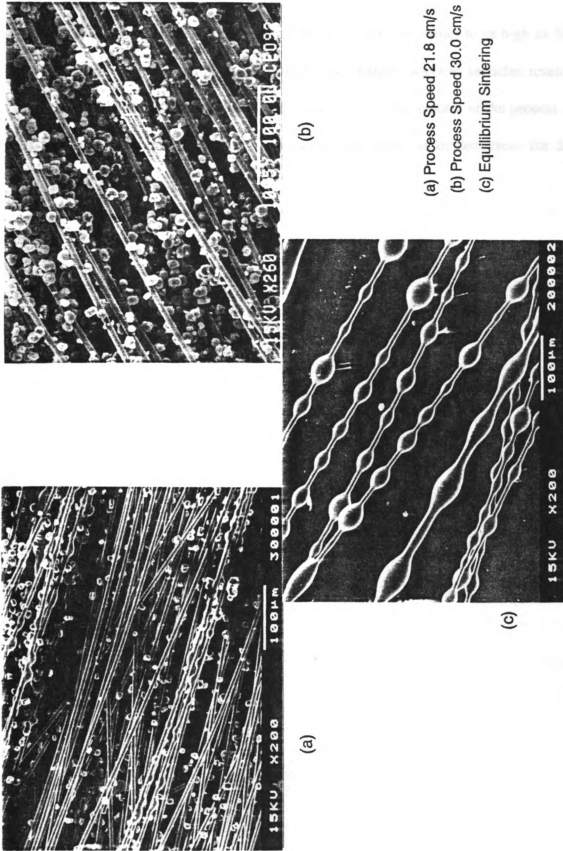


Figure 5.4 SEM Micrographs of AS4 Carbon - Polyamide Prepreg

fraction of matrix on fibers can be controlled from very low values to as high as 50%. The motion of spread fibers in an aerosol of tribo-charged polymer particles results in a uniform deposition of particles by electrostatic forces. The success of the process also lies in the uniform impregnation of particles on the fibers as evident from the SEM micrographs in Figure 5.4.

Chapter 6

Conclusions

The conclusions that can be drawn as a result of this study are summarized below.

1. A new high speed prototype of the powder prepreg process has been designed, constructed and demonstrated successfully. This prototype operates at the economically viable speed of 20 cm/s or greater, which is an order of magnitude greater than the operating speed of the first laboratory version of the process. The high speed powder prepreg process is capable of producing impregnated reinforcing fibers with any desired volume fraction of matrix to manufacture prepreg tapes where each fiber is intimately wetted by the polymer matrix.
2. The process does not use any external means to charge the polymer particles, instead it relies on the natural phenomenon of tribocharging of the polymer particles to acquire high charge to mass ratios and then adhere to the reinforcing fibers to produce prepreg tape. The process is also independent of matrix viscosity and does not use any solvents.
3. The process is composed of four unit operations: i) spreading the fiber tow; ii) generating an aerosol of polymer powder; iii) impregnating the polymer particles onto

spread fibers; and iv) sintering the particles in place. The original laboratory prototype process was designed for a line speed of 2 cm/s with each stage of operation placed in a horizontal configuration. Operations (ii) & (iii) were performed in a single stage known as the aerosolizer. Research into the behavior of the aerosolizer led to the design of an impregnating system for the scaled-up version in which aerosol generation and particle impregnation on the fibers were separated.

4. A vertical counter current impregnation chamber has been designed for impregnating polymer particles onto the spread fiber tow. This chamber offers flexibility in speed of operation and makes impregnation independent of aerosol generation. It provides the requisite residence time for the powder particles and the fiber filaments to come in contact while requiring a small area of floor space.

5. Research into the aerosolization characteristics of various polymer powders in a small-scale setup made the powder process suitable for different matrix systems and provide the design parameters for the scaled-up version. As a result of these studies the concept of a gas distributor ring was developed which can control the rate of aerosol generation and entrainment. Entrainment studies indicated at least a tenfold increase in the rate of aerosol generation and entrainment with the use of this gas distributor. Further, in order to direct the aerosol to the impregnation chamber a nozzle for dry nitrogen gas was used.

6. In view of the high speed of operation, a sophisticated process control strategy was adopted. Steady state operation required that the speeds of the motors be synchronized. A tension controller which is very fast responding in sensing the fluctuations in the fiber motion and very effective in controlling the motor speeds accordingly has been incorporated.

The following recommendations for future work are made as a result of this investigation.

- (i) An improvement in the sintering operation will be required for prepregging higher temperature material. The existing oven should be replaced with a tubular heater with three zone temperature controller. Alternatively, an infra red heater with proper temperature control for heating prepreg in a vertical mode could be considered.
- (ii) Maintaining the same fiber tow spread width from the time it leaves the spreader to the time it enters the heater is often an operational challenge. A means to keep the spread width constant in this vertical configuration should be explored.
- (iii) Investigate the physics of powder impregnation on the spread fibers in the impregnation chamber.
- (iv) Incorporate an in-line sensor and feedback system which can control the volume fraction of the matrix on the prepreg.

Bibliography

Bibliography

- [1] Grayson, M., Encyclopedia of Composite Materials and Components, *John Wiley & Sons*, 1983.
- [2] Iyer, S. R., Drzal, L. T., "Dry Powder Processing of Thermoplastic Composites", *Fifth Technical Conference [Proc]*, p 259-266, American Society of Composites, 1990.
- [3] Lee, S. M., International Encyclopedia of Composites, *VCH*, 1990.
- [4] Iyer, S. R., "Continuous Processing of Unidirectional Prepreg", *Ph.D. Dissertation*, Michigan State University, 1990.
- [5] Padaki, S., "Powder Processing of Composite Prepreg Tape : Particle Size Effects", *M.S. Thesis*, Michigan State University, 1992.
- [6] Taylor, G. J., "Method of Impregnating a fibrous Textile Material with a Plastic Resin", *U.S. Patent 429105*, Sept. 1981.
- [7] O'Connor, J. E., "Reinforced Plastic", *U.S. Patent 4680224*, July 1987.
- [8] Turton, N., and McAinsh, J., "Thermoplastic Compositions", *U.S. Patent 3785916*, 1974.
- [9] Moyer, R. L., "Methods of Making Continuous Length Reinforced Plastic Articles", *U.S. Patent 3993726*, Nov. 1976.
- [10] Cogswell, F. N., Hezzell, D. J., and Williams, P. J., "Fiber-Reinforced Compositions and Methods for Producing Such Compositions", *U.S. Patent 4559262*, Dec. 1985.
- [11] Lind, D. J., and Coffey, V. J., *U.K. Patent 1485586*, 1977.
- [12] Clemans, S. R., Western, E. D., and Handermann, A. C., "Thermoplastic Hybrid Yarns for High-Performance Composites", *Materials Engineering*, Vol 105, 27-30, 1988.
- [13] Chary, R. R., Hirt, D. E., "Powder Coating of Carbon Fibers Using Aqueous Foam", *37th International SAMPE Symposium [Proc]*, 1992
- [14] Price, R. V., "Production of Impregnated Roving", *U.S. Patent 3742106*, June 1973.

- [15] Muzzy, J., et. al, "Electrostatic Prepregging of Thermoplastic Matrices", *SAMPE Journal*, vol. 25, No. 5, September/October 1989.
- [16] Allen, L. E., Edie, D.D., Lickfield, G. C., and J. R. McCollum, "Thermoplastic Coated Carbon for Textile Preforms", *J. Thermoplastic Composite Materials*, 1, p371-379, 1988.
- [17] Iyer, S. R., Ball, M., and Drzal, L. T., "Production of Composite Materials by Powder Processing", *ICCM[Proc]*, 1991.
- [18] Geldart, D. (editor), Gas Fluidization Technology, *John Wiley & Sons*, 1986.
- [19] Iyer, S. R., and Drzal, L.T., "Behavior of Cohesive Powders in Narrow Diameter Fluidized Beds", *Powder technology*, 57(2), p127-133, 1989.
- [20] Visser, J., "Van der Waals and Other Cohesive Forces Affecting Powder Fluidization", *Powder Technology*, 58 p1-10, 1989.
- [21] Gallo, C. F., and Lama, W. L., *J. of Electrostatics*, 2, p145-150, 1976.
- [22] Bailey, A. G., "Electrostatic Phenomenon During Powder Handling", *Powder Technology*, 37 p71-85, 1984.
- [23] Bauch, H., "Influence of Chemophysical Powder Properties on Charging and Applying Processes By Electrostatic Powder Coating"
- [24] Harper, W. R., "Contact and Frictional Electrification", OUP 1967
- [25] Fuchs, N. A., The Mechanics of Aerosols, *The Macmillan Co.*, 1964
- [26] Perry, R. H., Green, D. W. (editors), Perry's Chemical Engineers' Handbook, Sixth Edition, *McGraw Hill Book Company*, 1984.
- [27] Iyer, S. R., Drzal, L. T., "Method and System for Spreading a Tow of Fibers", *U.S. Patent Nos. 5,042,111 and 5,042,122* , 1991.
- [28] Iyer, S. R., Drzal, L. T. and Jayaraman, K., "Method for Fiber Coating with Particles", *U.S. Patent Nos. 5,123,373; 5,102,690 and 5,128,199* 1992.
- [29] Beddow, J. K., Particulate Science and Technology, *Chemical Publishing Co. Inc.*, 1980
- [30] Frenkel, J., *J. Physics U.S.S.R.*, 9, 385, 1945.
- [31] Camile Data Acquisition and Control System - Software and Hardware Manuals, Dow Chemical Co.
- [32] Speed and Tension Controller Operating Instructions, IDC Corp.
- [33] Single Turn Absolute Optical Position Encoder, Installation manual, Allen Bradley Co.